BENTHAM SCIENCE

CrossMark

Current Medical Imaging

Content list available at: https://benthamscience.com/journals/cmir

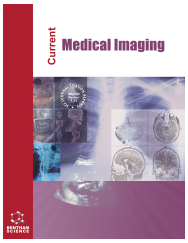

REVIEW ARTICLE

MRI Insights in Breast Imaging

Alessia Angela Maria Orlando[1], Paola Clauser[2], Calogero Zarcaro[1,*], Fabiola Ferraro[1], Calogero Curatolo[1], Maria Adele Marino[3] and Tommaso Vincenzo Bartolotta[1]

[1]*Department of Biomedicine, Neuroscience and Advanced Diagnostic (Bi.N.D.), University Hospital "Policlinico P. Giaccone", Palermo, Italy*
[2]*Department of Biomedical Imaging and Image-guided Therapy, Medical University of Vienna, Vienna, Austria*
[3]*Department of Biomedical Sciences and Morphologic and Functional Imaging, University of Messina, Messina, Italy*

Abstract:

In the world, breast cancer is the most commonly diagnosed cancer among women. Currently, MRI is the most sensitive breast imaging method for detecting breast cancer, although false positive rates are still an issue. To date, the accuracy of breast MRI is widely recognized across various clinical scenarios, in particular, staging of known cancer, screening for breast cancer in high-risk women, and evaluation of response to neoadjuvant chemotherapy. Since technical development and further clinical indications have expanded over recent years, dedicated breast radiologists need to constantly update their knowledge and expertise to remain confident and maintain high levels of diagnostic performance in breast MRI. This review aims to detail current and future applications of breast MRI, from technological requirements and advances to new multiparametric and abbreviated protocols, and ultrafast imaging, as well as current and future indications.

Keywords: Breast cancer, Magnetic resonance imaging, Diffusion, BI-RADS, Screening, Chemotherapy.

Article History	Received: September 26, 2023	Revised: November 17, 2023	Accepted: December 22, 2023

1. INTRODUCTION

In the world, breast cancer is the most commonly diagnosed cancer among women. Early detection and accurate diagnostic and therapeutic management remain crucial for improved patient outcomes [1, 2]. Breast MRI is mainly used to screen for breast cancer in women at increased risk as well as cancers with known stages, and evaluate the response to neoadjuvant chemotherapy [1, 2]. Nowadays, Magnetic Resonance Imaging (MRI) is the most sensitive breast imaging technique. In more recent large-scale studies, its sensitivity has been reported to range from 75.2% to 100%, generally over 80%, with specificity ranging from 83% to 98.4% [3]. False-Positive Rates (FPRs) reported in recent MRI screening studies have been found to range between 5.2% and 9.7% based on BI-RADS scores [4 - 6]. Considering that MRI imaging findings often require a rather complex management, including MR-guided biopsies, this is one of the main issues that limit a more widespread use of the method. Inclusion of recently developed sequences in multiparametric protocols could aid in the reduction of the FPRs [7].

* Address correspondence to this author at the Department of Biomedicine, Azienda Ospedaliera Universitaria Policlinico "Paolo Giaccone" di Palermo, Palermo, Italy; E-mail: calogerozarcaro@gmail.com

The purpose of this paper was to provide an overview of the current status, research, and future applications of breast MRI by reviewing many aspects from technological advances to MRI protocols and clinical indications.

2. TECHNICAL REQUIREMENTS FOR BREAST MRI

It is widely recognized that high-field strength MR scanners (at least 1.5T) with gradients > 20 mT/m are required to obtain images at high spatial and temporal resolution, with the aim of detecting and characterizing small anomalies on MRI [1, 2]. Obtaining diagnostic quality images requires a multichannel (at least four channels)-dedicated breast coil. Both breasts are free to hang in the recesses of the coil while patients are in the prone position. Positioning patients as comfortably as possible is crucial to avoid motion artifacts and ensure good image quality [2, 7 - 9].

2.1. Insights from Technological Advances

2.1.1. Breast Dedicated Multichannel Phased-array Coils and Parallel Imaging

Phased-array multichannel coils take full advantage of modern parallel imaging (PI) techniques, which are robust methods for accelerating the acquisition of MRI data, acquiring

a small quantity of k-space data. The most modern breast dedicated coils have 16 channels or more, as well as occasionally axillary-specific channels. The Signal-to-Noise Ratio (SNR) and speed of image acquisition increase with the number of channels [7, 10, 11]. The most recent PI techniques have enabled the optimization of new MR sequences, such as the Ultrafast Dynamic Contrast-Enhanced (Ultrafast DCE) and high-resolution DWI sequences [12 - 14]. In particular, compressed sensing is an innovative method introduced in the field of signal processing, acquiring images with far fewer samplings than "needed", demonstrated to reduce scan times up to 50%, thereby offering accurate and high-resolution images and resolving the spatial /temporal trade-off [15].

2.1.2. 3T MRI Scanners

The high-field strength of the 3T MR scanners provides numerous opportunities for improving the quality of diagnostic images. Compared to 1.5T scanners, in the case of spatial resolution, potential improvements in SNR and data collection speed have been reported [16, 17]. Nevertheless, due to increasing field intensity, some potential but solvable limitations have been reported, such as magnetic susceptibility artifacts and increased T1 relaxation rates of breast tissues. Magnetic susceptibility effects that manifest at soft tissue/air interfaces, often along the breast's circumference at the breast-body junction, could be exacerbated by 3T scanners. The robustness of fat saturation is improved by the 3T's greater spectral separation of water and fat, potentially reducing these effects [18]. T1 increases from 1.5T to 3T in breast glandular tissue by about 100 msec. Consequently, T1 sequences might be optimized in order to maintain similar T1-weighting, for example by slightly increasing the TR, with a penalty of scan time or by slightly reducing the flip angle [19].

Earlier studies have suggested that 3T MR scanners provide improved imaging quality or diagnostic performance than 1.5T scanners [16, 17, 20 - 25]. Nevertheless, most of these studies have been retrospective or have involved small populations or specific clinical contexts [20 - 22].

In a recent prospective study performed by Dietzel *et al*., 982 patients undergoing breast MRI, based on standard indications, were randomized to one 3T or 1.5T scanner [26]. This research demonstrated comparably high diagnostic accuracy, without significant differences, between 1.5T and 3T breast MRI, suggesting that the initial reported benefits of 3T breast MRI could be attributed to study design or potential bias in favor of newer techniques [26].

3. BREAST MRI PROTOCOL

The standard breast MRI investigation includes typically a pre-contrast T2-weighted sequence and a Dynamic Contrast-Enhanced (DCE) sequence [1, 2, 7].

T2-weighted fast/turbo spin-echo with or without fat saturation and/or a Short Tau Inversion Recovery (STIR) or Spectral Pre-saturation with Inversion Recovery (SPIR) sequences are used for morphological evaluation. Furthermore, water-containing lesions have an intense signal, while most cancers show intermediate to lower signals than parenchyma because of their elevated cellularity and reduced water content. Only a few malignant lesions may present with very elevated signal intensity on T2-weighted sequences, such as mucinous or metaplastic carcinoma. These sequences also enhance perifocal or pre-pectoral edema, which is often related to malignancy and a poorer prognosis [27, 28].

DCE acquisition is obtained with a T1-weighted 3D spoiled gradient echo pulse sequence with or without fat saturation, performed before an immediate intravenous bolus of a Gadolinium (Gd)-containing contrast agent. This procedure is repeated several times after the contrast agent has been administered, as rapidly as possible for 5 to 7 min [29]. The recommended dose of contrast agent is 0.1 mmol/kg with an injection rate of 2 ml/s, followed by saline flushing of 20 ml, preferably using an automatic injector. After contrast material administration, 5-7 volumetric acquisitions, each at 60-90 sec, are obtained. Breast MRI should be able to identify all lesions that are 5 mm or larger and provide more precise information for morphological evaluation of lesions. If the image quality is high, lesions smaller than 5 mm can be detected and characterized. For these reasons, images are acquired in the axial plane, with a thickness $\leq$ 2.5 mm, and a pixel size or an in-plane resolution (FOV/matrix) of no more than 1 mm, necessitating a 300 mm FOV and a matrix of at least 300 mm x 300 mm. Modern MRI units and breast coils allow to obtain image reconstruction in any plane and considerably higher resolutions (1 mm isotropic and lower) without sacrificing acquisition time (beyond 90 seconds), allowing the evaluation of lesions, particularly the distribution of non-mass lesions [1, 7]. Post-processing techniques, such as subtraction images, maximum intensity projections, and time-intensity curves help radiologists identify, describe, and characterize mass and non-mass enhancements [30 - 32]. More recently, quantitative pharmacokinetic parameters, such as k_{trans} (a transfer constant that reflects the rate of transfer of contrast agent from the plasma to the tissue) and ke_p (a transfer rate constant that reflects the reflux of contrast agent from the extravascular extracellular space to the plasma compartment), have been demonstrated to improve the differential diagnosis among the breast lesions and even help distinguish between different breast cancer subtypes [33 - 35].

3.1. Insights on Breast MRI Protocols

3.1.1. Ultrafast DCE Imaging

The term "Ultrafast" DCE imaging refers to modern MR sequences, sharing a similar new approach of k-space filling that enables to image the inflow of a contrast agent with a high temporal resolution, also known by their commercial names, such as Time-resolved angiography with Stochastic Trajectories (TWIST), 4-Dimensional Time-Resolved magnetic resonance Angiography with Keyhole (4D-TRAK), Time-Resolved Imaging of Contrast Kinetics (TRICKS), and DIfferential Sub-sampling with Cartesian Ordering (DISCO) sequence [12, 36, 37].

Multiple phases (10-16) of Ultrafast DCE-MRI are captured continuously for roughly 60-90 seconds beginning simultaneously with the onset of contrast injection after a pre-contrast full k-space sample, for a total acquisition time of 102-120 seconds [12, 36 - 39]. Ultrafast sequences can be used in combination with the conventional DCE acquisition, which can result in a hybrid Ultrafast-DCE protocol (Fig. **1**).

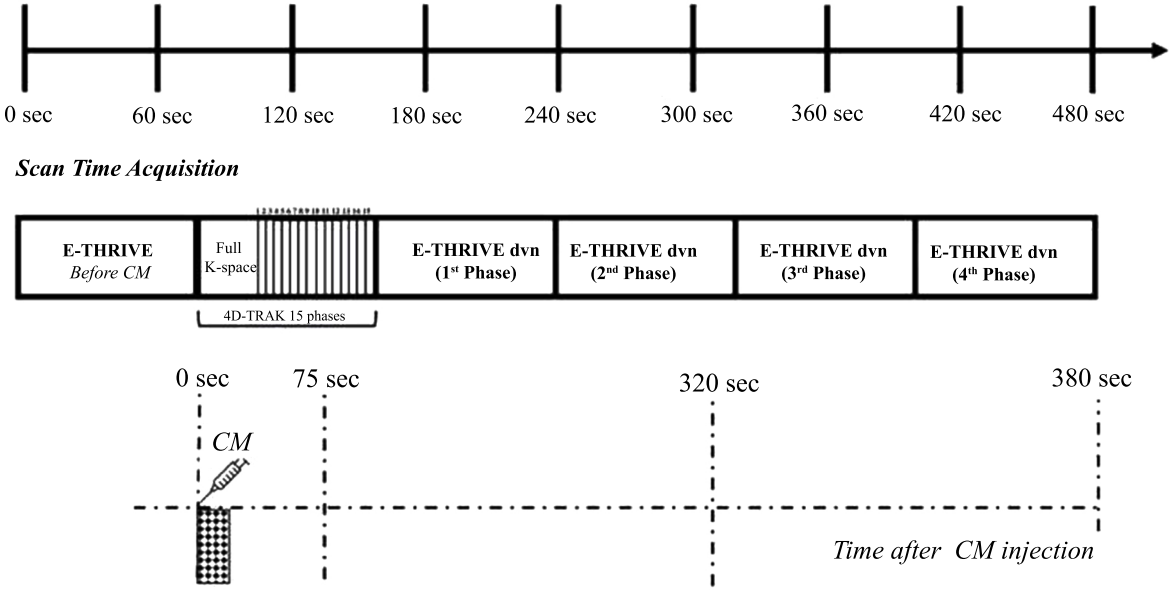

Fig. (1). An example of a hybrid protocol of Ultrafast and conventional dynamic contrast-enhanced sequences. DCE: dynamic contrast-enhanced.

In contrast to conventional DCE, Ultrafast images present moderate spatial resolution with in-plane resolution and thickness slightly superior, depending on the MR intensity field, number of channels of breast coils, and vendors (Table **1**) [12, 36 - 40]. The generation of a MIP series from the subtracted Ultrafast images provides a movie of contrast inflow in patients with cancer, and a "lightbulb" effect can be noticed, in which cancer enhances in an otherwise completely black breast [12, 31, 32, 36] (Figs. **2** and **3**). Early enhancement parameters generated from Ultrafast kinetic curves, such as time to enhancement (TTE) and maximum slope (MS), could be useful in breast lesion detection and characterization. TTE, the amount of time it takes for a lesion to become more visible after contrast has entered the descending aorta, may be used as a discriminatory tool since malignant lesions normally become more visible much sooner than benign lesions, usually within 10 seconds, whereas benign lesions typically take longer (on average >15 seconds) [7, 36 - 38]. The slope of the steepest part of the concentration curve (measured in mMol/sec) or the increase in relative enhancement between three adjacent time points divided by time (measured in percent relative enhancement per second) showed higher values in malignant than in benign breast lesions [37, 38].

Table 1. Acquisition parameters for ultrafast and conventional DCE sequences with different MR scanners.

Sequence	*Shin et al.*, European Radiology (2020)				*Onishi et al.*, Breast Cancer Research (2020)	
	Siemens Ultrafast Conventional DCE		*Philips* Ultrafast Conventional DCE		*GE* Ultrafast Conventional DCE	
	TWIST VIBE		4 D TRAK- 3D TFE	e THRIVE	DISCO	VIBRANT
In-plane resolution (mm x mm)	1.11 x 1.24	0.83 x 0.83	0,94 x 0,94	0.90 x 0.90	1.6 x 1.6	1.1 x 1.1
FOV	320 x 320 mm2	320 x 320 mm2	300 x 300 mm2	300 x 300 mm2	34 x 34 cm^2	34 x 34 cm^2
Matrix size	288x259	384 x384	320 x 320	332 x 332	212 x 212	300 x 300
TR (ms)	4.1	4.7	3.9	5.2	3.8	7.9
TE (ms)	1.3	1.7	2	2.4	1.1/2.2	4.3
FA (°)	10	10	12	12	12	12
Temporal resolution (s)	3.8	88	4.5	89	2.7- 4.6	~ 120
Parallel imaging factor	CAIPIRINHA 5	CAIPIRINHA 2	SENSE 4 (phase)× 2 (slice)	SENSE 3.2 (phase) × 1 (slice)	ARC 4 (phase) × 2 (slice)	ASSET 2 (phase) × 1 (slice)

Abbreviations: DCE=dynamic contrast enhacend, TWIST= time-resolved angiography with interleaved stochastic trajectories, VIBE = volume-interpolated breath-hold examination, TRAK = time-resolved MR angiography with keyhole, TFE = turbo field echo, eTHRIVE = enhanced T1-weighted high-resolution isotropic volume examination, DISCO= differential sub-sampling with cartesian ordering, Vibrant= volume imaging breast assessment, FOV= field of view, TR= repetition time, TE= echo time, FA= flip angle, CAIPIRINHA= controlled aliasing in parallel imaging results in higher acceleration, SENSE= sensitivity encoding, ARC= autocalibrating reconstruction for cartesian imaging, ASSET= array coil spatial sensitivity encoding.

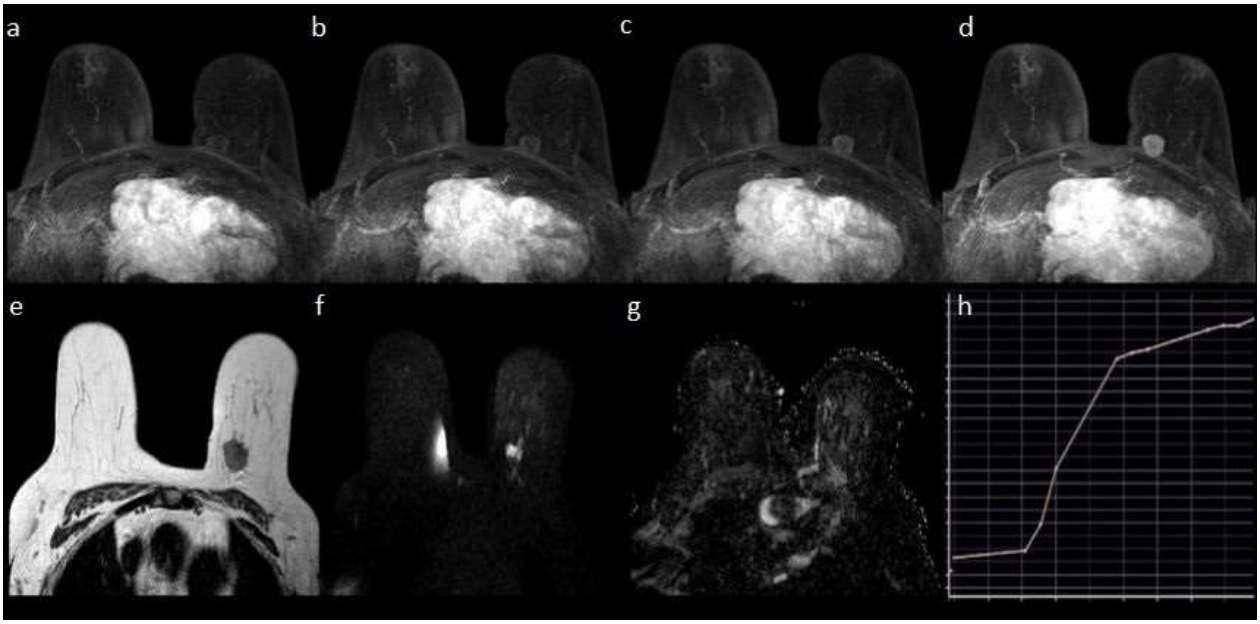

Fig. (2). A 73-year-old woman with a HER2-enriched invasive ductal carcinoma. (**a-d**) Maximum intensity projection (MIP) images derived from the Ultrafast series show a rounded mass, with irregular margins, in her left superior inner breast. Time to enhancement was judged at 0 sec., as the mass was already detectable, although with a rim moderate enhancement at the same time as the ascending aorta (**a**). In the following series, the enhancement progressively increases with a centripetal course (**b-d**) with a peak enhancement at 13.5 sec (**d**). The time-intensity curve derived from the Ultrafast sequence showed a rapid initial rise (**h**). FSE T2w images revealed perilesional and pre-pectoral edema (**e**); The b800 DWI sequence and ADC map showed a high intralesional restriction (**f-g**). Perilesional, pre-pectoral edema was also detectable as a high signal, posterior to the malignant hypointense malignant lesion, in ADC maps.

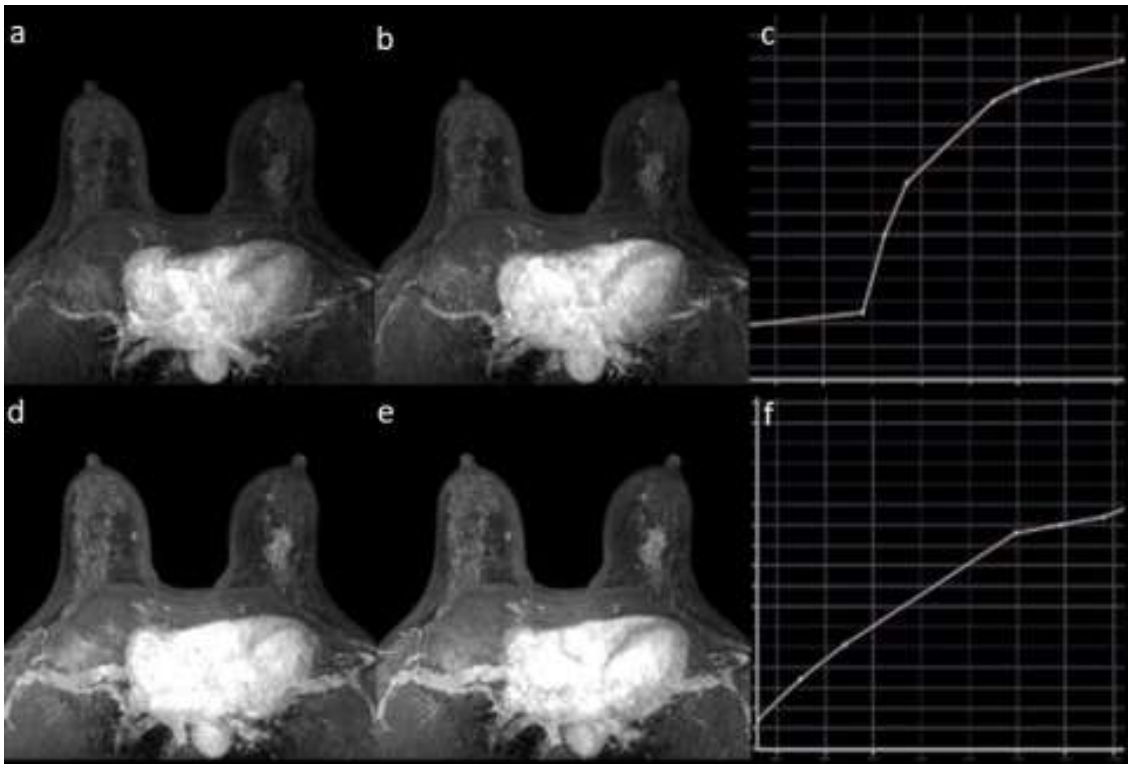

Fig. (3). A 45-year-old woman with a radial scar in her left upper central and a fibroadenoma in her inferior inner left breast. Maximum intensity projection (MIP) images derived from the Ultrafast series, at 9 sec (**a**) , 13.5 sec (**b**) , 18 sec (**d**) , and 22,5 sec (**e**) show the following findings: a large focal heterogeneous mass enhancement in the upper central left breast, with a TTE of 9 sec, and a time-intensity curve derived from Ultrafast sequence revealing a rapid initial rise (**c**) ; a sub-centimetric oval-shaped mass enhancement, with circumscribed margins, showing an early enhancement (with a TTE of 9 sec), and a time-intensity curve derived from Ultrafast sequence revealing enhancement as progressive (**f**).

Furthermore, the goal of the study conducted by Mann *et al*. was to make a comparison between MS and the BIRADS-defined curve type. The 199 enhancing lesions included were all detectable on the standard DCE sequence and TWIST, and the MS allowed for a considerably better separation of benign and malignant lesions than BIRADS curves (AUC 0.829 *vs*. AUC 0.692, respectively; p=0.036) [12].

Both these Ultrafast MRI-derived early enhancement parameters, TTE and MS, were also linked to histopathologic prognostic factors and tumour aggressiveness in breast cancer patients [38 - 40].

Furthermore, encouraging results were recently reported about the possible use of Ultrafast parameters in predicting pathologic response after neoadjuvant therapy [41]. In particular, in the single-centre study of Ramtohul *et al*., a wash-in slope of more than 1.6% per second was linked to higher pCR rates in the HER2-positive breast cancer subgroups (OR, 21.7; P = .02) and lower residual cancer burden in luminal HER2-negative and triple-negative breast cancer subgroups (OR, 11.0; P = .04) [42].

Despite these promising results, both DCE and Ultrafast-derived quantitative parameters' reproducibility needs to be improved [43], and further larger studies are needed.

3.1.2. Abbreviated Protocol

A typical full breast MRI study protocol takes between 17 and 40 minutes to complete. Decreasing image acquisition and reading time may help make breast MRI screening more widely available. In 2014, Kuhl *et al*. first looked into whether an abbreviated protocol (AP), consisting of just one pre- and one postcontrast acquisition and the resulting images and first postcontrast subtracted and MIP images, would be appropriate for breast magnetic resonance imaging (MRI) in a setting for breast cancer screening [31]. In their experience, obtaining an AP in 3 minutes, an expert radiologist's MIP image reading time of 3 seconds, and an NPV of 99.8% are all required to determine the absence of breast cancer. While interpretation of the whole AP, as with the FDP, provided identification of all malignancies with a reading time of less than 30 seconds [31].

Later, other authors investigated the application of MRI AP in breast cancer screening, and obtained similar results [44 - 50]. Comparing AP with full protocol, Oldrini *et al*. documented no appreciable variations between two readers' sensitivity and specificity, differently experienced in breast MR imaging; they reported significantly reduced reading time with AP for both reviewers (247 *vs*. 329 seconds and 59 *vs*. 142 seconds) [46]. Nevertheless, Grimm *et al*. reported a reduced overall sensitivity with their APs (AP 1: 86%, AP 2: 89%) compared to 95% sensitivity of the full protocol, but in both abbreviated protocols, the cancer missed was a recurrent invasive ductal carcinoma in a mastectomy patient on the chest wall. Surprisingly, there were no discernible differences between the AP and complete protocol interpretation times; the authors attributed this evidence to the lack of confidence of radiologists in interpreting MR images in the absence of traditional sequences [48].

Some studies have also included a T2 FSE in the AP, with or without fat suppression, and/or a STIR sequence [47 - 50]. In the study of Heacoch *et al*. the addition of the T2W sequence did not affect the cancer detection rate, and was considered helpful in 49.5% of cases, only for the least experienced reader (*vs*. < 8% of cases for the 2 more experienced readers) [47]. Missed cancers reported with AP were mainly non-mass enhancement (NME) or mass enhancement (ME) localized at the chest wall or near the axilla [47, 48].

The "Comparison of Abbreviated Breast MRI and Digital Breast Tomosynthesis in Breast Cancer Screening in Women with Dense Breasts" EA1141 trial, a randomized prospective multi-center study, enrolled 1444 women with dense breasts who underwent both abbreviated breast MRI and DBT [51, 52]. Shorter breast MRIs had greater rates of invasive cancer detection (11.8 per 1000 *vs*. 4.8 per 1000, p=0.002) and sensitivity for invasive cancer or DCIS than DBT (95.7% *vs*. 39.1%, p=0.002). Although AP MRI showed significantly lower specificity than DBT (86.7% *vs*. 97.4%, P<0.001), the PPV of biopsy was not statistically significantly different compared to DBT (19.6% - 21/107 patients *vs*. 31.0% - 9/29 patients, p=0.15). Furthermore, no differences in additional imaging recommendation rates were noted [52]. Despite these encouraging findings, significant reservations still exist regarding the utility of breast MRI as a screening technique in individuals who are not at high risk. Breast MRI facilities are less accessible than mammography facilities, and lengthier travel times may be related to sociodemographic variables, including living in a rural area and having less education. Additionally, Gadolinium-Based Contrast Agents (GBCAs) must be administered intravenously (IV) for breast MRI [53, 54].

3.1.3. Multiparametric Protocol

The term multiparametric protocol refers to the combination of functional MRI techniques in breast imaging, such as diffusion-weighted imaging and MR spectroscopy (MRS), with the aim of overcoming limitations in specificity and improving diagnostic accuracy in breast cancer [33, 55, 56].

3.1.3.1. Diffusion-weighted Imaging (DWI)

Diffusion-weighted imaging (DWI), which was first used in the middle of the 1980s, is now more frequently used in clinical MRI protocols, particularly to look into neurological illnesses and cancer [57]. A T2-weighted (b0) Echo-Planar Imaging (EPI) sequence is subjected to motion-sensitizing gradients (b factors) in order to produce images using DWI, which is based on the Brownian movement of water molecules in tissues. A reliable quantitative illustration of the diffusivity of water molecules is provided by the apparent diffusion coefficient (ADC) maps derived from the DWI sequence, obtained with at least 2 *b factor* ponderations (given in s/mm2). The term "apparent" diffusion coefficient refers to the fact that the water diffusion coefficient in tissues is subject to a variety of influences, including non-Gaussian diffusion and IntraVoxel-Incoherent Motion (IVIM), which is the perfusion of capillary networks [58].

Because of their intralesional decreased diffusion of water caused by increased cell density, the majority of malignancies exhibit higher signal intensity at DWI and low signal in ADC maps [7, 59]. ADC values are generally lower in malignant lesions ($0.8–1.3x10^{-3}mm^2/sec$) than in benign ones ($1.2–2.0x10^{-3}mm^2/sec$) [60]. Nevertheless, T2 black-out artifacts due to fibrotic components or viscous environment can lead to low ADC values in benign lesions, such as in radial scar/complex sclerosing lesions and complicated cysts, and T2 shine-through artifacts due to necrotic/cystic components can provide high ADC values in breast cancer [61, 62].

Due to its lesion characterization capabilities, DWI is emerging as an essential part of multiparametric breast MRI. There are still some challenges in the routine use of quantitative DWI, which are especially related to the lack of standardization of imaging approaches across institutions, MRI scanner vendors, and measurement methods to obtain ADC values (from b values applied to the definition of a region-of-interest). Standardization seems crucial to avoid variable results and inappropriate image interpretations, improve reproducibility, and support widespread utilization [63].

Dorrius *et al*. performed a meta-analysis including 26 studies to evaluate the effect of the choice of b values on ADC values of breast lesions and the characterization of breast lesions. They concluded that while ADC of breast lesions was significantly affected by the choice of b values (the higher the b value used to calculate the ADC, the lower the ADC becomes), the latter did not impact sensitivity and specificity, recommending b values to be 0 and 1.000 s/mm for optimal differentiation between benign and malignant lesions [64].

While the majority of research concurs that ADC values are not impacted by MR field strength but rather by applied b values, even without significantly affecting accuracy, some differences in the selection of b-values have been noted. The majority of the literature [7, 56, 60, 65 - 68] suggests b-values between 0 and 800 sec/mm2 for clinical usage, suggesting an optimal balance between adequate diffusion weighting and tolerable signal-to-noise ratio. In particular, several authors have hypothesized that while 0 and 1000 s/mm2 are the theoretically ideal combination of b values for the brain, where diffusion is rather slow, 0 and 800 s/mm2 constitute the ideal pair for the majority of bodily tissues, including the breast [69 - 71].

To consistently and accurately assess ADC, it is necessary to standardize acquisition parameters and breast tumor tissue selection techniques [by defining a Region of Interest (ROI)]. The impact of various defined breast tumor tissue selection procedures on the accuracy of ADC to identify breast lesions was examined in a comprehensive review and meta-analysis that included 61 studies using DWI scanned on 1.5 and 3.0 Tesla and utilizing b-values 0/50 and 800 s/mm2. The authors categorized 4 ROI positioning methods, which are as follows: 1) whole breast tumor tissue selection; 2) subtracted whole breast tumor tissue selection; 3) circular breast tumor tissue selection; and 4) lowest diffusion breast tumor tissue selection. The last three methods avoid areas with necrosis, cysts, or hemorrhages. None of these techniques for selecting breast tissue has been found to perform better than the others at separating benign from malignant breast lesions. However, there has been found substantial variation between investigations, and information on scanning settings has been found to be frequently incomplete [72]. Wielema *et al*. investigated the reproducibility of various breast tumor tissue selection techniques, concluding that fixed-size techniques displayed excellent reproducibility and that the most practical technique for use in clinical practice is the one that has a central fixed breast tumor tissue volume of 0.12 cm3 [73].

The conventional spin-echo DWI image quality may be negatively affected by ghosting artifacts, geometric distortions, and blurring, which typically occur due to the single-shot echo planar imaging readout method [14]. The new readout-segmented DWI sequence, based on multi-shot echo planar imaging, was demonstrated to mitigate ghosting artifacts with a slight decrease in SNR, even with 2-mm in-plane resolution [14, 74, 75]. Nevertheless, this last technique requires a longer acquisition time. More recently, parallel imaging solutions have been introduced, including the simultaneous multi-slice (SMS) acquisition based on the blipped 'Controlled Aliasing in Parallel Imaging Results in Higher Acceleration' (blipped CAIPIRINHA) technique, which demonstrated to fill these gaps between scan times and spatial resolution [13, 76 - 79].

Furthermore, breast MR imaging at 3T enabled to obtain higher-resolution DWI by reducing the field of view and concentrating on a specific area of the breast with an in-plane resolution of 0.8 mm [80, 81]. Reduced field of view EPI, according to Park *et al*., can produce images with better lesion conspicuity and SNR than read-out-segmented EPI [82].

Moreover, the breast imaging community is currently using DWI as an add-on sequence in addition to DCE imaging [83] (Figs. **4** and **5**), and its role has been investigated and encouraged in various application fields: lesion detection and characterization, prognosis, axillary lymph node status, and evaluation and prediction of therapeutic response [58, 61, 62, 83 - 89]. Dietzel *et al*. recently investigated whether DWI could be used to replace the DCE sequence's delayed phase (DP), assuming that both are influenced by extracellular space properties that provide overlapping physio-pathological information. Their goal was to shorten and simplify current breast MRI practice without losing diagnostic information [61]. Adding ADC values to the evaluation of the initial phase (IP) of the DCE sequence led to an increase in diagnostic accuracy of 13.4% ($p = 0.002$), reaching higher AUC values (0.877). Identical diagnostic results were obtained from the multiparametric assessment including IP, DP, and ADC, but requiring an additional 5 min of scanning time [61]. Several studies have suggested an important role of ADC values before, during, and at the end of Neoadjuvant Therapies (NAT) [62, 84 - 89]. Particularly, compared to responder patients, non-responder patients had tumors with greater baseline ADC values (which were also linked with higher stages of necrosis) [62, 84, 85]. Due to cell death and the ensuing decrease in cellularity during NAT, the ADC values of breast cancer generally increase, and these changes typically occur before tumor size reduction [62, 86 - 88]. Additionally, Woodhams R *et al*. demonstrated DWI to be more accurate than DCE (96% *versus* 89%) at identifying residual tumor after NAT [89].

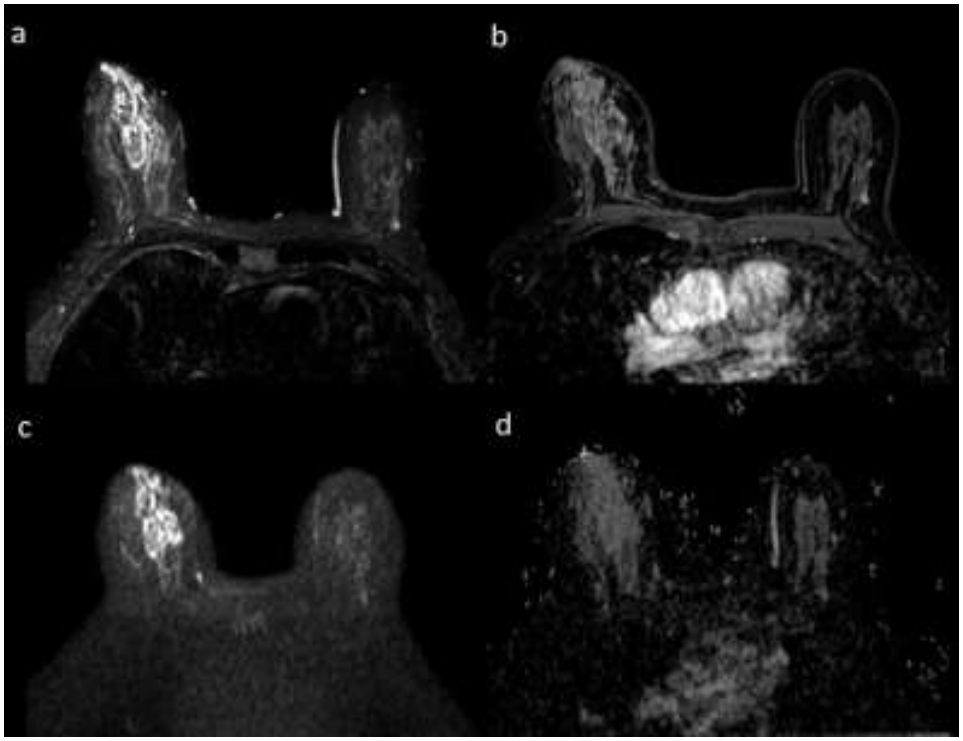

Fig. (4). A 65-year-old woman with a multi-orificial brown nipple discharge in her right breast. STIR sequence (**a**) revealed a unilateral duct ectasia with segmental distribution in the upper inner quadrant of the right breast. DCE sequence (**b**) showed a non-mass-like enhancement, with a "clustered rings" pattern and segmental distribution. The same area revealed a high signal in both DWI sequence (**c**) and ADC maps (**d**). Histological diagnosis confirmed chronic periductal mastitis.

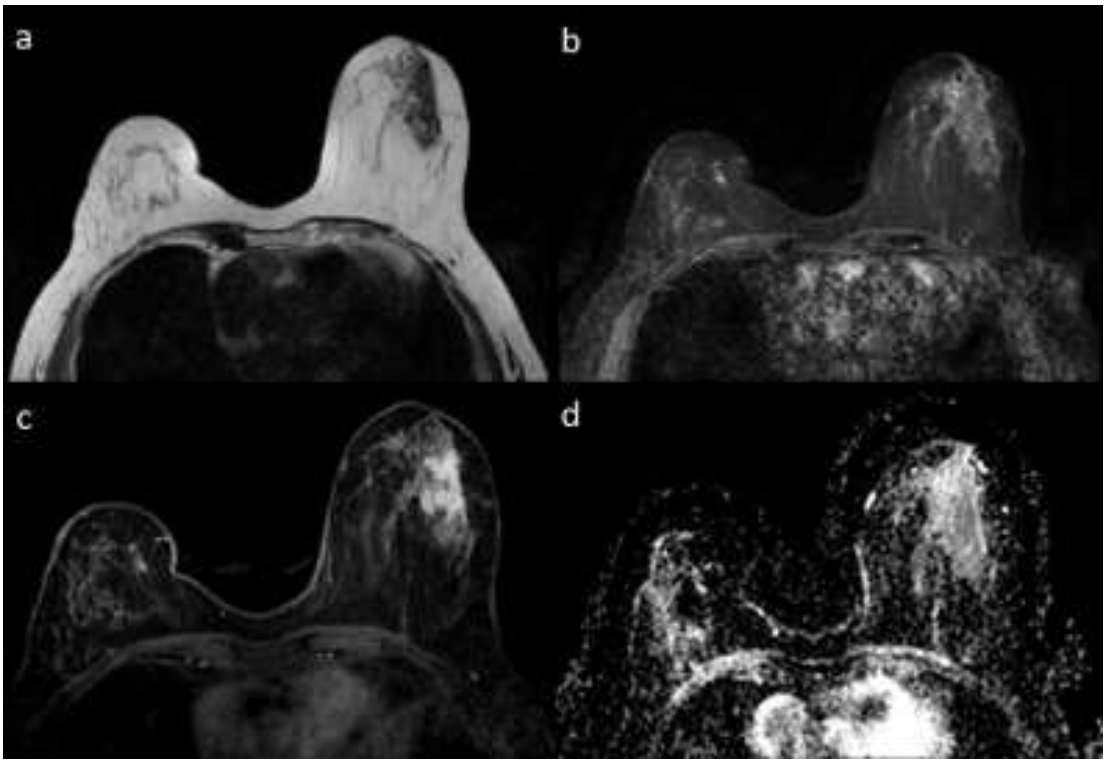

Fig. (5). A 63-year-old woman with a history of invasive ductal carcinoma in her right breast underwent a breast MRI for a developing asymmetry revealed on her upper outer left breast at mammography without abnormalities detectable on breast sonography. Asymmetry was confirmed on T2 FSE (**a**) and STIR (**b**) images, with a corresponding heterogeneous non-mass-like enhancement with segmental distribution on DCE sequence (**c**) and abnormal diffusion restriction confirmed by ADC maps (**d**). Histological diagnosis: low-grade *in situ* ductal carcinoma.

Nevertheless, as mentioned above, the most frequent and well-known obstacles to DWI's inclusion in the Breast Imaging Reporting and Data System (BI-RADS) lexicon were the wide variation in thresholds reported for ADC in differentiating between benign and malignant breast lesions [60, 64] and the absence of standardized protocols and ADC measurement methods [90].

With the aim to overcome these issues, in the last few years, the European Society of Breast Radiology (EUSOBI) established an International Breast DWI working group, which developed the first consensus recommendations, with the aim to standardize the application of DWI sequence in breast MRI protocols, from the acquisition parameters to the ADC values measurement methods. The minimum acquisition requirements are described as follows: an EPI-based sequence acquired with axial orientation, a field of view covering both breasts and fat saturation (SPAIR is recommended), TR $\geq$ 3000 ms and the minimum possible TE (obtained by optimizing the receiver bandwidth), in-plane resolution of $\leq$ 2×2 mm^2 with slice thickness $\leq$ 4 mm, a parallel imaging factor $\geq$ 2 with the aim to reduce distortion (loss in signal/noise ratio can be counterbalanced by increasing the number of excitations), 2 *b* values (more is optional), the lowest 0 s/mm^2 (however not exceeding 50 s/mm^2) and the highest 800 s/mm^2. Experts recommend obtaining the ADC value by drawing a region of interest (ROI) on the darkest part of the lesion on the ADC map, containing at least 3 voxels and avoiding necrotic, noisy, or non-enhancing lesion voxels. Then, the mean ADC value within the ROI should be reported with the units in 10-3 mm2/s. On the basis of ADC measurements and lesion appearance, the working group also proposed a descriptive classification of diffusion level in lesions, including very low ($\leq 0.9 \times 10^{-3}$ mm^2/s), low ($0.9–1.3 \times 10^{-3}$ mm^2/s), intermediate ($1.3–1.7 \times 10^{-3}$ mm^2/s), high ($1.7–2.1 \times 10^{-3}$ mm^2/s), and very high ($> 2.1 \times 10^{-3}$ mm^2/s), remarking that lesion characterization should always be done in conjunction with all morphological and functional information derived from all other imaging data and not solely based on diffusion level [71].

Finally, the survey recently conducted by the EUSOBI International Breast Diffusion-Weighted Imaging working group revealed that most breast radiologists use nowadays DWI as part of their routine protocol, including lesion characterization (using an ADC threshold of $1.2\text{-}1.3 \times 10^{-3}$ mm^2/s) and assessment of response to chemotherapy as common indications. Nevertheless, report integration of DWI results is not uniform, with most radiologists mentioning hindered diffusivity in the MRI report, and only 57% reporting ADC values [91].

Other new advanced modelling approaches for DWI are currently under investigation, classified as “Gaussian models”, such as Diffusion Tensor Imaging (DTI), and “non-Gaussian models”, such as Intra-Voxel Incoherent Motion (IVIM) and Diffusion Kurtosis Imaging (DKI) [14, 33, 55].

3.1.3.2. Diffusion Tensor Imaging (DTI)

Diffusion tensor imaging (DTI) builds on the DWI technique by using six or more additional diffusion-encoding directions. It is possible to calculate anisotropic diffusion within each voxel using a diffusion tensor, which is a matrix of directional diffusion coefficients. According to the hypothesis, the ductal and glandular microarchitecture in breasts directs and clearly defines the motion of water molecules [14, 33, 55, 92 - 94].

The two primary parameters that DTI quantifies are mean diffusivity (MD) and fractional anisotropy (FA). FA describes the level of anisotropy, whereas MD reflects the average anisotropy [92 - 95]. Diffusion anisotropy was found to be much lower in breast tumors than in normal tissues by Partridge *et al*. [92, 93]. This finding may be due to changes in the organization of the tissue microstructure. Baltzer *et al*. discovered that although FA did not have an incremental value when compared to ADC, DTI enabled them to see the microanatomical distinctions between benign and malignant breast cancers [96]. Finally, a more recent study containing the largest prospective cohort of patients evaluated DTI features of 238 suspicious breast lesions detected on MRI, and concluded higher FA to be significantly associated with malignancy (OR = 1.45, p = 0.007) [97].

Other authors have investigated the correlation between DTI parameters and breast cancer prognostic factors. Onaygil *et al*. found lower FA values in ER-negative breast cancer ($p< 0.05$) and that Ki-67 showed a significant, negative correlation with FA, whereas Ozal *et al*. demonstrated that patients with lymph node metastasis and/or lymphovascular invasion and/or histologic grade 3 tumors had statistically significantly low MD. The main limitations of this “Gaussian method” are non-standardized protocols, fitting methods, and ROI placements, and not always optimal image quality related to the echo-planar imaging sequence.

3.1.3.3. Intravoxel Incoherent Motion (IVIM)

Through the IVIM effect, blood flow in randomly oriented capillaries simulates a diffusion process and can be used to detect tissue diffusivity and microcapillary perfusion without the need for contrast agents [57]. Recent research suggests that the IVIM effect can be exploited to gather useful data on the microvasculature and tissue microstructure that contribute to the characterisation of breast masses [98 - 100]. The perfusion fraction (or blood volume fraction of the vasculature), tissue diffusion coefficient, and pseudodiffusion coefficient related to water flow inside the microvasculature are the three main parameters of the IVIM.

Perfusion fraction of malignant tumors was shown to be substantially higher than that of benign lesions, according to Liu *et al*. [101]. Other authors investigated the role of IVIM in the differentiation of different breast cancer subtypes and molecular prognostic factors; in the study of Kim *et al*., low tissue diffusivity was significantly observed in high Ki-67 tumours and luminal B (HER2-negative) tumours [102]. Lastly, Cho *et al*. found that the pseudodiffusion parameter significantly differentiated RECIST responders from non-responders [103].

However, it has taken longer for the potential of IVIM to be understood since it requires very good image quality and an accurate estimate of IVIM parameters linked to perfusion. Recent improvements in MR technology and software have

increased the signal-to-noise ratio in IVIM MRI, making an improvement in image quality easier to achieve [104]. The poor repeatability and reproducibility of IVIM parameters, which are largely a result of their dependence on acquisition factors, including b-values, TE, and fitting methods [104 - 108], may yet be overcome. To solve these problems, standardized IVIM data collection and reliable IVIM fitting must be developed.

3.1.3.4. Diffusion Kurtosis Imaging (DKI)

Diffusion kurtosis imaging quantifies the deviation of tissue diffusion from a Gaussian pattern; in living tissues, due to barriers from complex tissue structures, Brownian incoherent motion and microperfusion or blood flow demonstrate non-Gaussian phenomena [109]. The diffusion kurtosis imaging technique, sensitive in the breast imaging competition to intracellular structures, like membranes and organelles, provides a diffusion heterogeneity index sensitive to the tumor microstructure by acquiring additional, higher b-value images, in the order of b = 1000-3000 s/mm^2 and at least 15 diffusion gradient directions [110, 111]. The mean kurtosis (MK) and mean diffusivity (MD), two parameters of the DKI that give microscopic information on the water diffusion's departure from a Gaussian distribution, are corrected for kurtosis [112].

The investigation of breast tumors using DKI has become an important research area [113 - 119]. The diagnostic performance of DKI and its applications remain controversial. Some studies have demonstrated a substantially higher sensitivity and specificity compared to ADC values for breast cancer diagnosis [120, 121]. In particular, in the study of Sun *et al*., kurtosis coefficients were positively linked with tumor histologic grade and Ki-67 protein expression and were considerably greater in malignant lesions than benign lesions (1.05 0.22 *vs*. 0.65 0.11, respectively; p.0001) [121]. However, Palm *et al*. discovered that DKI did not enhance the performance of differentiating breast tumors in clinical protocols [114]. Additionally, there was disagreement over DKI parameters. Park *et al*. claimed that there was no discernible difference between benign and malignant tumors [115], although the majority of research has revealed breast cancer to have a higher MK and a lower MD than benign lesions [113, 117, 119]. Finally, a recent meta-analysis including 867 malignant and 460 benign breast lesions found that breast cancer showed a significantly ($P < 0.001$) higher MK and lower MD than benign tumors, and that MK ($P = 0.006$) can further differentiate invasive ductal carcinoma from ductal carcinoma *in situ* [112]. DKI shares the same limits as other Gaussian models, including a lack of standardization in data acquisition, protocol parameters, and fitting methods.

3.1.3.5. Proton MR Spectroscopy

MRS is a non-invasive method that reflects a tissue's chemical composition. The ability to see spatially localized signal spectra with spectral peaks reflecting the structure and concentration of several detectable metabolites enables the identification of various tissue states, such as normal, benign, malignant, necrotic, or hypoxic tissue, by selecting a region of interest [122].

Although the method for *in vivo* MRS is not yet standardized, it may be useful in the context of multiparametric MRI.

Proton (^{1}H) MRS, performed as single-voxel or multi-voxel MRS, offers the greatest sensitivity and simplest data acquisition, with the greater contribution provided by the detection of choline peak. The choline peak, observed at 3.32 ppm, is the result of many different choline-containing metabolites, such as free choline, phosphocholine, phosphoethanolamine, and glycerophosphocholine [122 - 124].

In breast cancer, the elevated total choline peak reflects increased cell density in the tumor and cell membrane turnover, serving as a biomarker for differentiating malignant and benign breast lesions [125 - 127]. A meta-analysis, conducted by Baltzer and Dietzel, including 19 studies with a total of 1193 patients, found for ^{1}H-MRS a pooled sensitivity and specificity of, respectively, 73% and 88%. No significant influences of field strength (3.0 T or 1.5 T), multivoxel over single-voxel techniques, or qualitative *versus* quantitative MRS measurements, were reported, whereas main limitations were found in small breast tumors and non-mass-enhancing lesions [128]. Montemezzi *et al*. reported analogue specificity results, reaching also a sensitivity of 90%, considering only invasive cancers and mass lesions ≥1 cm and excluding lesions close to the skin or pectoral muscle [129].

^{1}H-MRS could also play a potential role in the early assessment of the response to NAT. Preliminary small sample size studies suggested a correlation between a reduction in choline peak and response to NAT, due to treatment-induced alterations in cell proliferation, which could be captured before any changes in tumor size [130, 131]. Nevertheless, the recent ACRIN 6657 MRS clinical trial found discordant results, with no evidence of significant ability to predict both pathological or radiologic responses for choline peak. However, the authors have found numerous limitations in collecting analyzable data, including variability in the placement of the MRS voxel within or encompassing the tumor, leading to a definitive sample size of only 29 cases, insufficient to accurately evaluate 1H-MRS measurements as a predictor of response to NAT [132].

Besides choline metabolites, lipid metabolites are detectable with ^{1}H-MRS and this has been evaluated in *in vivo* MRS studies; cancer showed higher water concentrations and lower methylene lipid peaks at 1.3 ppm [133, 134].

In addition to the 1.3 ppm fat peak, Thakur *et al*. recently used MRS to identify 5–6 lipid peaks [135]. They looked into the usefulness of different lipid concentrations for prognosis prediction as well as for differentiating between molecular subtypes (luminal A/B *vs*. others; luminal A *vs*. others) and characterizing breast distinguishing lesions. Additionally, they discovered that a clearer separation of the lipid peaks at 2.1 ppm and 2.3 ppm was revealed with greater field strength (3T) and the STEAM sequence, enabling the calculation of polyunsaturated and saturated fatty acid fractions.

Nowadays, MRS studies suffer from a large variability related to MR field strength (1.5T or 3T) and adoption of breast receiver coils, sequence performance (PRESS – Point Resolved Spectroscopy or STEAM – Stimulated Echo Acquisition

Mode), acquisition parameters (TR, TE, *etc*.), parallel imaging factors, adoption of single- or multi-voxel approaches, voxel size and position software, and quantitative methods available for spectra analysis (EPRM - External Phantom Reference Method or IWRM - Internal Water Reference Method). Other limitations include a relatively long acquisition time (10–15 minutes) and the possibility of a low-quality spectrum in breast MRS related to poor shimming and chest wall motion [133].

3.1.3.6. Emerging MRI Parameters

Recently, novel MRI parameters have been developed in research applications, including sodium imaging (^{23}Na MRI), phosphorus spectroscopy (^{31}P MRS), Chemical Exchange Saturation Transfer (CEST) imaging, Blood Oxygen Level-Dependent (BOLD) MRI, Hyperpolarized MRI (HP MRI), and MR elastography [14, 33, 55].

^{23}Na MRI relies on the abundance of ^{23}Na in the body and on elevated tissue sodium concentration in malignant lesions due to disruption of the sodium-potassium pump in cell membranes. Sodium concentration also correlates well with the ADC of DWI [136 - 138].

Phosphorus spectroscopy (^{31}P MRS) identifies the signals of catabolites and phospholipid precursors involved in the metabolism of cell membranes [139]. Increased levels of phosphocholine (PC) and phosphoethanolamine (PE) have been seen in a variety of solid tumors, including breast cancer, in both *in vitro* and *in vivo* 31P MRS studies. Today, despite evidence that 31P MRS can be utilized for breast cancer detection, tumor staging, and therapeutic response monitoring, clinical application is restricted due to the scarcity of ultrahigh-field magnets and the need for specialized coils [140, 141].

Chemical Exchange Saturation Transfer (CEST) imaging enables visualization of chemical exchange processes between protons bound to solutes and surrounding bulk water molecules, providing for example images through the Amide Proton Transfer (ATP) effect. In some studies, ATP-CEST has been found to be able to differentiate benign and malignant breast tumors [142, 143]. Although in preclinical studies, other applications of CEST imaging in breast cancer have been investigated, such as dynamic CEST imaging after the administration of glucose (glucoCEST), which could depict the kinetics of glycolysis, typically enhanced in malignant lesions [144].

Blood Oxygen Level-Dependent (BOLD) micro-environmental perfusion and hypoxia can be assessed using MRI. For imaging tissue hypoxia, which is associated with tumor growth, angiogenesis, treatment resistance, local recurrence, and metastasis, deoxyhemoglobin is a paramagnetic molecule that functions as an intrinsic BOLD contrast agent [145 - 147].

Hyperpolarized MRI (HP MRI) allows a quick, non-invasive investigation of tumour metabolism by exploiting exogenous contrast agents that have been "hyperpolarized". The most popular probe for HP MR research is (^{13}C) pyruvate, which has a long T1 relaxation time, is quickly taken up by the cell, and processed during glycolysis, tricarboxylic acid, and amino acid production [148]. It is polarized to obtain enhancements of the ^{13}C nuclear MR signals. The ability to distinguish between benign and malignant tumors and to assess the course of cancer using real-time measurements of the relative transformation of pyruvate into lactate and alanine with HP MRI has been demonstrated in preclinical studies [149, 150].

MR elastography (MRE) images a low-frequency acoustic wave as it propagates throughout tissue to characterize the biomechanical characteristics of breast tissue, including variations in stiffness, or to record known prognostic factors, such as desmoplasia associated with breast cancer, stiffening of the surrounding stroma, and necrosis [44, 45]. Currently, MRE research and techniques are still developing [45].

3.1.4. Noncontrast-enhanced Abbreviated MRI of the Breast

Emerging imaging techniques show the possibility to pave the way for a new avenue, the so-called "non-contrast enhanced abbreviated MRI of the breast", especially diffusion-weighted imaging (DWI) techniques. Although DWI increases specificity, it currently only has therapeutic utility when used in conjunction with DCE-MRI and not as a stand-alone test [151, 152]. Particularly discordant results are now being reported. Baltzer *et al*. found comparable AUC values for both techniques when they compared full diagnostic protocol dynamic contrast-enhanced MRI (DCE-MRI) with non-contrast MRI with DWI in 113 patients with BI-RADS 4 and 5 lesions [153]. In a retrospective investigation by McDonald *et al*., three readers who were blind to the CE-MRI results assessed unenhanced sequences, and the average performance showed a low sensitivity (45%) but a better specificity (91%), suggesting only a potential utility in a supplemental screening context [154].

However, Bu *et al*., who investigated the relationship between DWI and Turbo Inversion Recovery Magnitude (TIRM), recently discovered encouraging evidence. An inversion pulse's subsequent turbo spin echo sequence is the independent part of the Turbo Inversion Recovery Magnitude (TIRM) measurement that is taken into account. In contrast to DCE-MRI, which showed no significant differences, DWI combined with TIRM was shown to be a safe, sensitive, and useful alternative for screening women with dense breasts. It also showed higher accuracy (AUC= 0.935) and sensitivity (93.68%) for breast cancer detection than MG (AUC = 0.783, sensitivity = 46.32%) [155].

4. IMAGE EVALUATION

For image evaluation and diagnostic interpretation, the Breast Imaging Reporting and Data System (BI-RADS) created by the American College of Radiology is widely recommended [1, 2, 7, 90]. Radiologists are required to report the clinical indication, the MRI sequences, and post-processing methods adopted, as well as the quantity and type of contrast agent used. It is important to note the breast composition and Background Parenchymal Enhancement (BPE). In particular, BPE (Fig. **6**) has been widely studied in different settings and observed to be related to higher abnormal interpretation rates, although there has not been a discernible decrease in the sensitivity and rate of cancer detection in women, according to various studies

looking at the impact of BPE on diagnostic performance [156]. At the DCE sequence, any findings should be described accordingly with the BI-RADS lexicon (Table **2**; Fig. **7 - 9**) as masses (space-occupying lesions), non-mass enhancement (NME) (areas of enhancement without a clear space-occupying lesion present) or focus (a dot of enhancement so small that it cannot be otherwise characterized; its shape and margin cannot be seen clearly enough to be described). An accurate description of any other non-enhancing findings or associated features, relative to the nipple, skin, chest wall, and axillary lymph node, should be added. The report's conclusion should include a final BI-RADS category (ranging from 0 to 6) and a consequent practical recommendation [157].

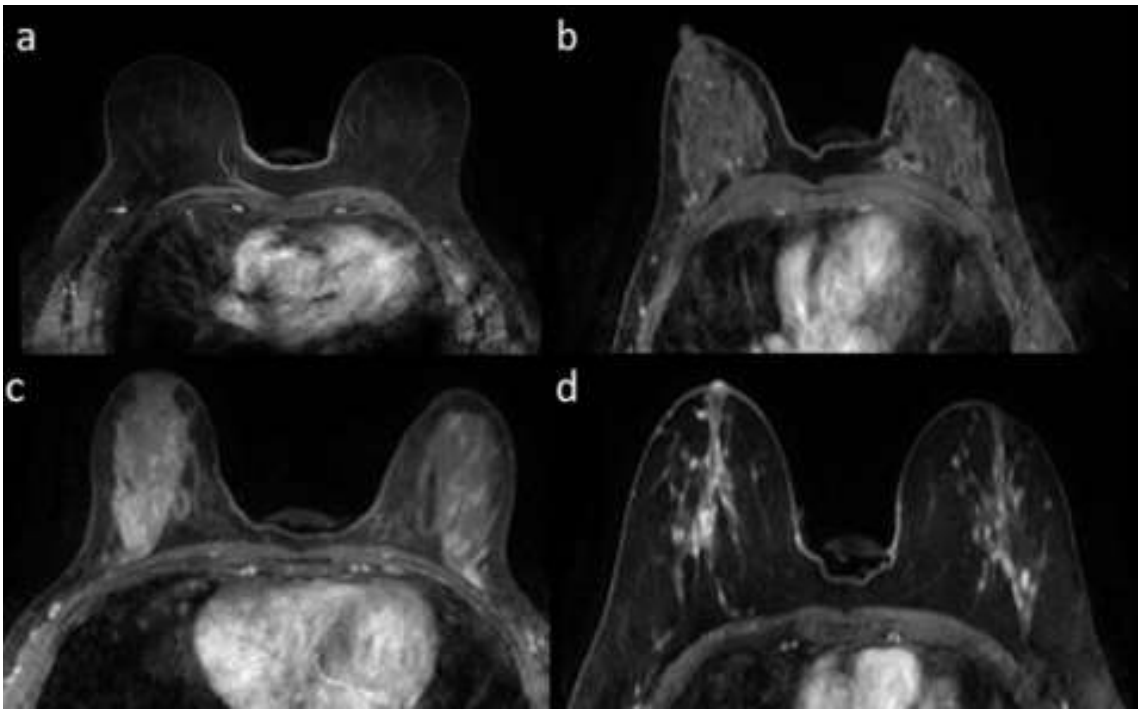

Fig. (6a-d). Background parenchymal enhancement: (**a**) minimal, (**b**) mild, (**c**) moderate, (**d**) marked.

Table 2. MRI BI-RADS lexicon: findings and descriptors.

Findings	Feature	Terms
Focus	-	-
Masses	Shape	Oval Round Irregular
-	Margin	Circumscribed Not circumscribed - Irregular - Spiculated
-	Internal enhancement characteristics	Homogeneous Heterogeneous Rim enhancement Dark internal septations
Non-mass enhancement	Distribution	Focal Linear Segmental Regional Multiple regions Diffuse
-	Internal enhancement patterns	Homogeneous Heterogeneous Clumped Clustered ring

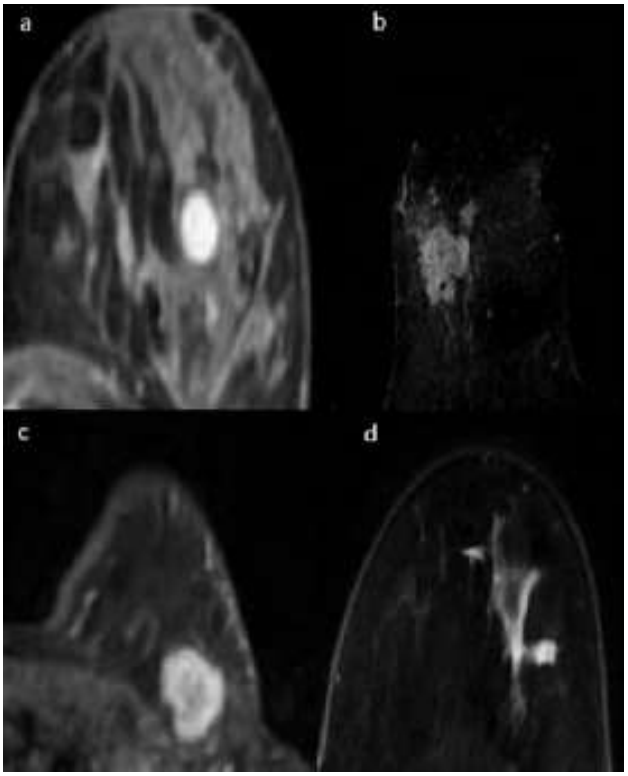

Fig. (7a-d). Mass enhancement – internal enhancement patterns: (**a**) homogeneous (fibroadenoma); (**b**) heterogeneous (invasive ductal carcinoma high-grade); (**c**) rim enhancement (invasive ductal carcinoma); (**d**) dark internal septations (fibroadenoma).

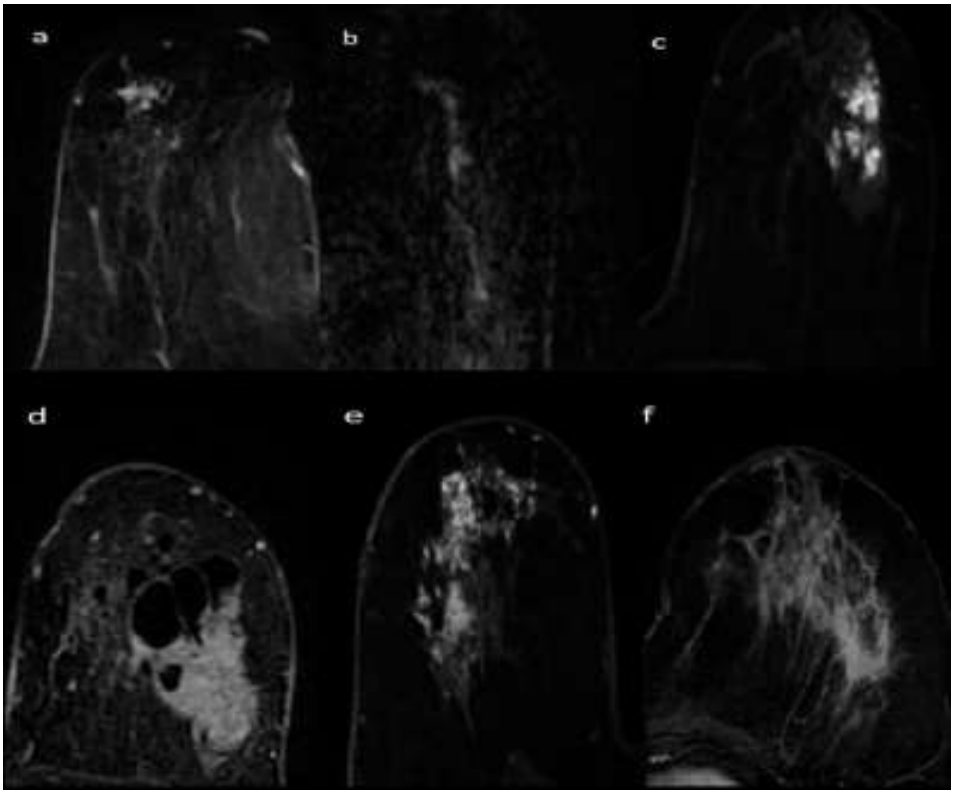

Fig. (8a-f). Non-mass enhancement – distribution: (**a**) focal (invasive ductal carcinoma); (**b**) linear (ductal carcinoma *in situ*); (**c**) segmental (ductal carcinoma *in situ* low grade); (**d**) regional (invasive ductal carcinoma); (**e**) multiple regions (invasive ductal carcinoma high-grade); (**f**) diffuse (inflammatory breast cancer in invasive ductal carcinoma high-grade).

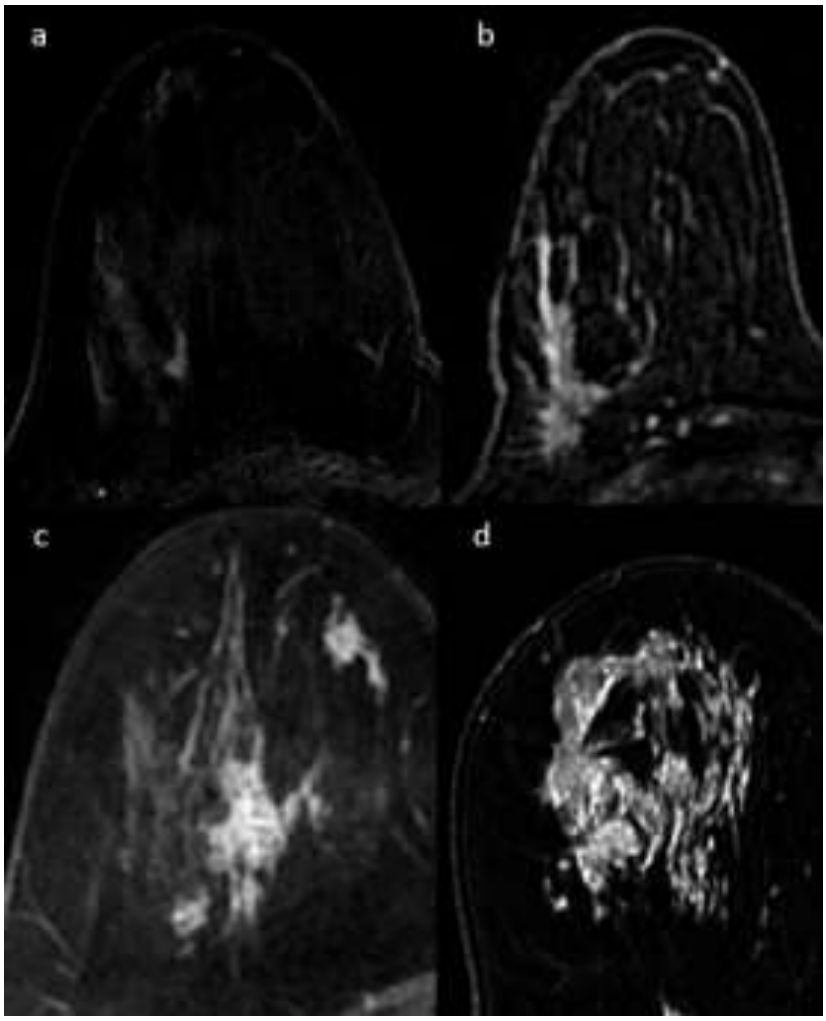

Fig. (9a-d). Non-mass enhancement - internal enhancement patterns: (**a**) homogeneous (sclerosing adenosis); (**b**) heterogeneous (radial scar); (**c**) clustered rings (ductal carcinoma *in situ*); (**d**) clumped (ductal carcinoma *in situ*).

Most breast cancers manifest as a mass typically with irregular shape and margin, heterogeneous or rim enhancement patterns, with or without wash-out detectable in the delayed DCE phase of time/intensity curves [158, 159]. Nevertheless, some malignant lesions may appear as masses with circumscribed margins, such as triple negative (frequently rounded) or mucinous carcinoma (sometimes with gradual enhancement pattern and often with elevated ADC values) [160, 161].

NME characteristics are typically less specific than mass characteristics [158, 162]. Recently, Aydin *et al*., retrospectively analyzing 129 NME, found that at multivariate logistic regression, only segmental distribution and diffusion restriction were associated with malignancy [163].

4.1. Insights from Breast MR Imaging Evaluation

Despite its fundamental role in standardizing and structuring reports, the BI-RADS lexicon does not provide clinical decision rules. However, the recently released Kaiser score, which integrates five distinct diagnostic BI-RADS lexical criteria (margins, SI-time curve type, internal augmentation, and presence of edema) in an easy-to-read tree flowchart, provides such a clinical decision rule [164 - 166]. In a recent study, the Kaiser score was able to rule out cancer in more than 45% of contrast-enhancing lesions that had previously been categorized as BI-RADS 4, potentially preventing needless biopsies [167].

5. INSIGHTS FROM CURRENT AND FUTURE CLINICAL APPLICATIONS

We have, herein, reviewed current known and already established indications [1, 2], looking at more recent evidence and resuming future indications and direction [168].

5.1. Staging Before Treatment Planning

An accurate preoperative staging is necessary in cases of newly diagnosed breast cancer in order to determine the extent of the cancer and to optimize the treatment plan. Preoperative breast MRI is unquestionably crucial in determining the extent of primary cancer as well as any additional malignant foci that may exist, identifying multicentric and contralateral disease. It is also crucial in determining whether the nipple, skin, and/or chest wall are involved as well as any local nodal metastases.

Several advantages and consequent limitations of breast cancer staging with MRI are still debated. Invasive interval cancers are thought to be more likely to develop in the postoperative period in people who are young, have tumors that do not express hormone receptors, or have dense breasts [169, 170]. Furthermore, patients with lobular carcinoma have been found to have the highest rate of accurately diagnosed extra ipsilateral or contralateral foci [171].

The Pre-Operative MRI of the Breast (POMB) trial results, which assessed the accuracy of incremental preoperative breast MRI findings, suggested that empirical AUC for the incremental findings in the entire MRI group was 85%, with a PPV of 74% (95% CI 60-84%), in 39 patients with MRI-related changes of initial treatment plans, and 27% (95% CI 14-44%) in 39 patients without [172]. Due to true positive and false positive incremental findings, the conversion rate from breast conservative surgery to mastectomy in the ipsilateral breast was comparable to that reported by Houssami *et al*. in their meta-analysis involving 19 preoperative investigations [172, 173].

According to a recent meta-analysis by Houssami *et al*. [174], the main debated concern regarding the utilization of breast MRI for BC staging is the potential for increased odds of receiving ipsilateral mastectomy and contralateral prophylactic mastectomy, with the exception of patients with invasive lobular carcinoma, who showed a decreased likelihood of reoperation (OR 0.65), though not significantly.

The European Network for the Assessment of Imaging in Medicine (EuroAIM) has approved the MIPA study, a large-scale observational multicenter international prospective analysis. The aim was to compare the surgical and clinical endpoints of two groups of patients, respectively, *i.e*., those who have undergone (MRI group) and not (noMRI group) breast preoperative MRI according to local practice. Researchers hypothesized that MRI reduces the reoperation rate, not being responsible for additional mastectomies compared to conventional imaging [175]. Recently published results demonstrated an additional planned mastectomy rate of 11.3% in the MRI group. Notably, in 14% of the noMRI group and 22% of the MRI group, mastectomy was previously planned based on conventional imaging. The fact that MRI was commonly used in this last group of patients who were already candidates for mastectomy as a confirmation procedure may have contributed to the 11% rise in mastectomy rates noted in the breast MRI group. Additional very relevant evidence of this study was that the MRI group had a considerably lower reoperation rate among women who underwent conserving surgery (8.5% *versus* 11.7%, p 0.001) [176].

5.2. Screening of High-risk Women

According to the American Cancer Society and the American College of Radiology, the term “high risk” refers to women who have a lifetime risk of more than 20%, including patients with genetic mutations (such as *BRCA1, BRCA2, PALPB2, TP53, PTEN, CHECK2, CDH1, ATM,* and *STK11*) or who have received mantle radiotherapy before the age of 30. For this patient group, annual screening MRI, in adjunct to mammography, is not only recommended but strongly advised by several societies [177, 178]. Breast MRI plays a crucial role for this patient group, as evidenced by the fact that it is sensitive enough to detect breast cancer in high-risk patients (sensitivity varies from 75–100%) [177 - 183]. Previous studies have reported that women with a BRCA mutation have a 60-85% cumulative lifetime risk of developing breast cancer, with 44.7% of cases being identified by MRI rather than mammography and more than half being less than 10 mm in size [179]. Breast MRI had a much greater cancer detection rate in high-risk women than mammography (21.8 malignancies per 1000 women screened *vs*. 7 per 1000), according to Lo *et al*. [180]. Radiation can have harmful effects on people who carry the BRCA1 mutation. Recent studies suggest that mammography be given a second look when patients undergo annual breast MRIs because there is no evidence that mammography increases the rate of cancer diagnosis in all high-risk people under the age of 40 [180, 184 - 186].

5.3. Screening of Intermediate-risk Women

According to the American Cancer Society and the American College of Radiology, women who have a lifetime risk of breast cancer between 15% and 20%, a personal history of cancer, dense breasts on mammography, or a history of high-risk lesions at biopsy (specifically, atypical ductal hyperplasia, atypical lobular hyperplasia, and lobular carcinoma *in situ*) are considered to be at “intermediate risk” [177]. Although the American Cancer Society did not recommend annual breast MRI screening in this patient group, further research backed this advice.

In a recent large cohort retrospective analysis, 2637 women with various increased breast cancer risk indicators had their screening breast MRI CDRs analyzed. With a CDR of 12 per 1000 and 15 per 1000 examinations, respectively, and no statistically significant difference for either when compared to the high-risk category, the authors concluded that screening breast MRI should be taken into consideration for women with a personal history of breast cancer or high-risk lesions [181].

Women with lobular carcinoma *in situ* benefit more than those with atypical lobular hyperplasia or ADH from screening MRI cancer detection rates, which are reported in the literature to vary from 10.5 to 22.7 malignancies per 1000 exams. Nevertheless, MRI may be responsible for unnecessary increases of biopsies and/or follow-up examinations recommended for benign lesions, with a PPV of biopsies performed ranging from 13% to 28.6% [187 - 190].

According to several studies, screening MRI cancer detection rates for women with a prior history of breast cancer range from 1.9 to 30.1 malignancies per 1000 exams, with a PPV of conducted biopsies ranging from 10% to 75.8% [187 - 194]. Furthermore, in patients with a history of cancer who have dense breasts or if the cancer was discovered before the age of 50, updated ACR guidelines recommend selective MRI surveillance [178].

5.4. Dense Breasts

Breasts on mammography are classified by BI-RADS as almost entirely fatty (category a), scattered areas of

fibroglandular density (category b), heterogeneously dense (category c), or extremely dense (category d) depending on the ratio of radiopaque tissue (fibroglandular tissue, FGT) to radiolucent tissue (fat). 'Dense' breasts is the term most frequently used to describe the latter two groups. Histologically, areas of collagen and epithelial glandular components, such as ducts and terminal duct lobular units, constitute radiopaque FGT [195 - 197].

Marked breast density may mask cancers on mammography [198 - 200] being responsible for decreased mammographic sensitivity and specificity [201], and consequently interfering with the goals of screening mammography programs, which namely are early detection and cost-effectiveness.

Mammographic breast density is also considered an independent risk factor for breast cancer. Since 1976, the year in which the first researches were published by Wolf *et al*. [202, 203], several further studies have suggested a strong positive association between dense breasts and the increased risk for breast cancer [199, 204, 205].

The benefit of supplemental imaging methods for a tailored breast cancer screening of women with dense breasts is nowadays widely debated. Over the last several years, multiple imaging modalities have been proposed, including breast MRI.

A systematic review evaluated diagnostic performance, cancer detection and recall rates of DBT, hand-held and automated breast ultrasound, and MRI when added to mammography of dense breasts. The authors found that, among women with dense breasts, MRI had a sensitivity rate of 75–100%, specificity of 78–94%, and a PPV of 3–33%, and when added to mammography screening, it detected 3.5–28.6 additional cancers per 1,000 women, but has been found to be associated with a recall rate of 12–24% [31, 179, 206, 207]. Nevertheless, they noted that women in studies selected for the systematic review likely had higher breast cancer risk than the general population of women with dense breasts.

The dense trial study group investigated the role of supplemental MRI screening for women with extremely dense breast tissue, including 4783 women with normal results on screening mammography. Supplemental MRI detected an additional 16.5 cancers/1,000 screens in the first round. The interval cancer rate was significantly lower in the MRI group (0.8/1000 *vs*. 5/1000). On the other hand, the PPV of MRI prompted biopsy was 26.3% and 0.1 women who underwent MRI % had either an adverse event or a serious adverse event during or immediately after the screening [5].

Nevertheless, adding biennial MRI to biennial mammography, as was performed in the DENSE trial, the cost-effctiveness goals of screening programs are far from being reached. Alternative strategies are thus needed [208, 209].

Further evidences were provided by the ECOG-ACRIN EA1141 study, which included 1444 women with dense breasts (BI-RADS category C and D) that underwent for screening with both DBT and abbreviated MRI. According to their results, additional contribution of X-ray-based breast imaging was very limited and abbreviated MRI showed similar results as the standard MRI protocol, used within the DENSE trial [52].

Consequently to the evidences of DENSE trial study and ECOG-ACRIN EA1141 study, the European Society of Breast Imaging (EUSOBI) group has recently drawn up new recommendations for screening women with extremely dense breasts [210]. According to these recommendations, MRI should be offered as a supplemental imaging method in this group of patients, from age 50 to 70, at least every 4 years, preferably every 2 to 3 years. The EUSOBI group also underscored that, even in the absence of national programs that offer MRI screening as part of national healthcare, women should be informed about this recommendation.

5.5. Evaluation of Response to Neoadjuvant Treatments (NAT)

NAT represents the recommended method in patients with locally progressed (stage II or III) and triple negative breast cancers. To evaluate response to NAT physical exam, mammography, US, and MRI have all been used. Among these, MRI is the most accurate method in distinguishing post-treatment fibrosis from residual tumor after NAT [211 - 213].

Early assessment of response to NAT is crucial, considering that a poor response may induce a change in the chemotherapeutic plan. In the Sheikhbahaei's study, DG-PET/CT imaging performed better than MRI for intra-NAC assessment; however, MRI performed better overall after NAC was finished but before surgery, with a considerably higher sensitivity (0.88 *vs*. 0.57) [214].

MRI evaluation of NAT response is affected by several factors, including breast cancer subtype (superior accuracy in triple-negative and HER-2 positive tumors than luminal ones), as well as presence of non-mass enhancement at pre-treatment and type of chemotherapy used (lower accuracy of NAT including taxanes has been reported) [215 - 218].

Overestimation of residual disease occurs in 6–19% of cases, as reported by Chen *et al*., and most causes include fibrosis/treatment changes and necrotic tumor [219, 220]. Whereas, underestimation occurs in 7–28% of cases and most causes include non-mass enhancement, late-enhancing foci, and tumors with non0concentric shrinkage [219, 220]. This evidence suggests that tailored interpretation strategy, taking tumor subtype and MRI phenotype into account, is needed.

Recently, the Response Evaluation Criteria in Solid Tumors (RECIST), the most generally adopted set of standardized criteria for response assessment, has recognized four categories of response: complete response, partial response, stable disease, and progressive disease [221]. Besides the only size assessment of target and non-target lesions, an early decrease in enhancement detected with pharmacokinetic modeling or time–signal intensity curve analysis and an early increase in ADC are also considered predictive of response [222 - 225].

Furthermore, while absence of late enhancement post-NAT is significantly associated with pathological complete response [Area Under the Curve (AUC): 0.85], quantification of residual enhancement may yield a higher sensitivity for pathological complete response with a loss of specificity [226, 227].

5.6. Occult Primary Breast cancer

The term occult primary breast cancer (OBC) is used when an axillary metastatic carcinoma without mammographic and ultrasonographic detection of a primary breast lesion occurs [228]. This condition, with an incidence of 0.1-3%, is probably secondary to micro-invasive breast cancer [229]. Compared to mammography or ultrasound, level I evidence showed MRI as much more sensitive in detecting a primary lesion, identifying 72% of cases of OBC [230]. If a breast MRI is negative, breast surgical treatment could be avoided, and the suggested therapeutic management, planned by a multidisciplinary team, is often axillary dissection and breast radiation therapy [231].

5.7. Problem-solving Tool

Although breast MRI has a high negative predictive value (NPV), the EUSOMA recommendation stated that MRI should not be used as an alternative for needle biopsy when it can be conducted and that MRI should be taken into consideration *in situations* where it is impossible to execute or specify a location for needle biopsy [2].

In non-calcified mammographically equivocal breast findings, such as asymmetry or architectural distortion, a recent meta-analysis reported a sensitivity of 99% with an NPV of 100% for breast MRI [178]. On the other hand, another sub-metaanalysis revealed that in patients with microcalcifications, the NPV of breast MRI was about 93%, which was insufficient to rule out cancer [232, 233].

Distinguishing local recurrence from post-treatment changes can be difficult in mammography; thus, breast MRI has gained widespread acceptance as a valuable problem-solving technique [234].

The frequency of recommendations for breast MRI to analyze ambiguous findings has drastically dropped after digital breast tomosynthesis (DBT) implementation; however, when such findings (mainly asymmetries) remain equivocal, breast MRI is a heplful supplementary tool [235 - 237].

5.8. Nipple Discharge

Despite that first guidelines and recommendation discouraged the routine usage of MRI in the clinical context of suspicious nipple discharge and advised ductography [1, 2], nowadays, it is widely recognized that MRI outperforms galactography, with a sensitivity for causal lesions of 92% *versus* 69% [237]. Nipple discharge cytology is constrained by a false negative rate of more than 50%, and galactography is an invasive procedure that may be painful and uncomfortable with a failure rate of up to 15% and a challenge differentiating between malignant and benign lesions [237 - 239]. Considering the superiority in accuracy of breast MRI in patients with suspicious nipple discharge, Pazironi *et al*. recently proposed a state-of-the art flowchart for the management of nipple discharge, incorporating breast MRI as a superior option [239].

6. INSIGHTS ON FUTURE DIRECTION

Future directions in breast MRI include ultra-high field MR scanners, breast low field MRI, breast PET/MRI, and radiomics and radiogenomics.

Efforts to obtain approval by U.S. Food and Drug Administration for clinical breast cancer applications using 7T MRI are actually ongoing. DWI, MRS, and other multiparametric modern techniques could gain from the growth of 7T MRI scanners. Besides obvious benefits in spatial and temporal resolution, technical advances have to be implemented with the aim to improve B1 homogeneity [240 - 242].

A really emerging approach is the low-field magnetic resonance imaging (typically with field strength well under 0.1T) that aims to provide diagnostic image quality, but with lower costs and environmental impact than high-field MRI [243]. A pilot study is currently being conducted to test, for the first time, a new method to image breast cancer using ultra-low field breast MRI with a 6.5 mT scanner. In detail, investigators are examining a new potential breast cancer MRI biomarker, the intrinsic T1rho dispersion signal [244]. T1rho dispersion is a tissue property which, at low frequencies, reflects protein content and composition of tissue and proton exchange between water and macromolecules. Researchers are expecting differences in T1rho dispersion between fat or fibroglandular tissues and breast cancer tissues [245].

The higher sensitivities of PET for axillary and internal mammary nodal metastases than standard breast MRI alone may be a benefit for dedicated breast PET/MRI [246]. While single-institution studies have revealed that PET/MRI enables to detect more metastases with a 50% reduction in total radiation exposure than PET/CT for whole-body imaging of breast cancer patients, a survival benefit has not yet been proven [246, 247].

Radiomics and radiogenomics represent a current research field stirring growing interest worldwide. The rapidly advancing field of artificial intelligence methods and their application to breast MRI suggests that radiomics is an emerging and promising tool for quantitative tumor assessment, which may enable the extraction of further quantitative data from radiological images. In particular, radiomic analysis may offer novel data by quantifying lesion heterogeneity that may be useful in clinical practice for the characterization of breast lesions, prediction of lymph node metastases, prediction of tumor response to systemic therapies, and evaluation of prognosis and recurrence risk in patients with breast cancer [248, 249]. The diagnostic and prognostic efficacy of radiomics applied to breast MRI has been examined in various published studies [250 - 259]. Despite the encouraging evidence, Codari *et al*.'s comprehensive analysis found that clinical practice is still far away from adopting AI applications due to the existing performance of such applications in breast MRI [260]. Further research is required to comprehend how the integration of radiomic data with other clinical and histopathological parameters could provide accurate models that could aid in clinical decision-making and patient management.

CONCLUSION

Currently, MRI is the most sensitive available breast imaging tecnhique for the detection of breast cancer. Technical development, further clinical indications, and new research

fields have emerged over recent years. Breast dedicated radiologists need to constantly update their knowledge and expertise with the aim to always remain confident and improve their diagnostic performance in this field of breast MRI.

LIST OF ABBREVIATIONS

MRI	=	Magnetic resonance imaging
FPRs	=	False-positive rates
Ultrafast DCE	=	Ultrafast dynamic contrast-enhanced
PI	=	Parallel imaging
SNR	=	Signal-to-noise ratio

CONSENT FOR PUBLICATION

Not applicable.

FUNDING

None.

CONFLICT OF INTEREST

The authors declare no conflict of interest, financial or otherwise.

ACKNOWLEDGEMENTS

Declared none.

REFERENCES

[1] Sardanelli F, Boetes C, Borisch B, *et al.* Magnetic resonance imaging of the breast: Recommendations from the EUSOMA working group. Eur J Cancer 2010; 46(8): 1296-316. [http://dx.doi.org/10.1016/j.ejca.2010.02.015] [PMID: 20304629]

[2] Mann RM, Kuhl CK, Kinkel K, Boetes C. Breast MRI: Guidelines from the European Society of Breast Imaging. Eur Radiol 2008; 18(7): 1307-18. [http://dx.doi.org/10.1007/s00330-008-0863-7] [PMID: 18389253]

[3] Mann RM, Kuhl CK, Moy L. Contrast-enhanced MRI for breast cancer screening. J Magn Reson Imaging 2019; 50(2): 377-90. [http://dx.doi.org/10.1002/jmri.26654] [PMID: 30659696]

[4] Chen SQ, Huang M, Shen YY, Liu CL, Xu CX. Application of abbreviated proto- col of magnetic resonance imaging for breast cancer screening in dense breast tissue. Acad Radiol 2017; 24(3): 316-20. [http://dx.doi.org/10.1016/j.acra.2016.10.003] [PMID: 27916594]

[5] Bakker MF, de Lange SV, Pijnappel RM, *et al.* Supplemental MRI Screening for Women with Extremely Dense Breast Tissue. N Engl J Med 2019; 381(22): 2091-102. [http://dx.doi.org/10.1056/NEJMoa1903986] [PMID: 31774954]

[6] Kuhl CK, Strobel K, Bieling H, Leutner C, Schild HH, Schrading S. Supplemental breast MR imaging screen- ing of women with average risk of breast cancer. Radiology 2017; 283(2): 361-70. [http://dx.doi.org/10.1148/radiol.2016161444] [PMID: 28221097]

[7] Mann RM, Cho N, Moy L. Breast MRI: State of the Art. Radiology 2019; 292(3): 520-36. [http://dx.doi.org/10.1148/radiol.2019182947] [PMID: 31361209]

[8] Konyer NB, Ramsay EA, Bronskill MJ, Plewes DB. Comparison of MR imaging breast coils. Radiology 2002; 222(3): 830-4. [http://dx.doi.org/10.1148/radiol.2223001310] [PMID: 11867809]

[9] Yeh ED, Georgian-Smith D, Raza S, Bussolari L, Pawlisz-Hoff J, Birdwell RL. Positioning in breast MR imaging to optimize image quality. Radiographics 2014; 34(1): E1-E17. [http://dx.doi.org/10.1148/rg.341125193] [PMID: 24428300]

[10] Marshall H, Devine PM, Shanmugaratnam N, *et al.* Evaluation of multicoil breast arrays for parallel imaging. J Magn Reson Imaging 2010; 31(2): 328-38. [http://dx.doi.org/10.1002/jmri.22023] [PMID: 20099345]

[11] Deshmane A, Gulani V, Griswold MA, Seiberlich N. Parallel MR imaging. J Magn Reson Imaging 2012; 36(1): 55-72. [http://dx.doi.org/10.1002/jmri.23639] [PMID: 22696125]

[12] Mann RM, van Zelst JCM, Vreemann S, Mus RDM. Is Ultrafast or Abbreviated Breast MRI Ready for Prime Time? Curr Breast Cancer Rep 2019; 11(1): 9-16. [http://dx.doi.org/10.1007/s12609-019-0300-8]

[13] Peng S, Guo Y, Zhang X, *et al.* High-Resolution DWI with Simultaneous Multi-Slice Readout-Segmented Echo Planar Imaging for the Evaluation of Malignant and Benign Breast Lesions. Diagnostics (Basel) 2021; 11(12): 2273. [http://dx.doi.org/10.3390/diagnostics11122273] [PMID: 34943509]

[14] Chhetri A, Li X, Rispoli JV. Current and Emerging Magnetic Resonance-Based Techniques for Breast Cancer. Front Med (Lausanne) 2020; 7: 175. [http://dx.doi.org/10.3389/fmed.2020.00175] [PMID: 32478083]

[15] Vreemann S, Rodriguez-Ruiz A, Nickel D, *et al.* Compressed Sensing for Breast MRI: Resolving the Trade-Off Between Spatial and Temporal Resolution. Invest Radiol 2017; 52(10): 574-82. [http://dx.doi.org/10.1097/RLI.0000000000000384] [PMID: 28463932]

[16] Kuhl CK, Jost P, Morakkabati N, Zivanovic O, Schild HH, Gieseke J. Contrast-enhanced MR imaging of the breast at 3.0 and 1.5 T in the same patients: Initial experience. Radiology 2006; 239(3): 666-76. [http://dx.doi.org/10.1148/radiol.2392050509] [PMID: 16549623]

[17] Spick C, Szolar DHM, Preidler KW, *et al.* 3 Tesla breast MR imaging as a problem-solving tool: Diagnostic performance and incidental lesions. PLoS One 2018; 13(1): e0190287. [http://dx.doi.org/10.1371/journal.pone.0190287] [PMID: 29293582]

[18] Schenck JF. The role of magnetic susceptibility in magnetic resonance imaging: MRI magnetic compatibility of the first and second kinds. Med Phys 1996; 23(6): 815-50. [http://dx.doi.org/10.1118/1.597854] [PMID: 8798169]

[19] Rakow-Penner R, Daniel B, Yu H, Sawyer-Glover A, Glover GH. Relaxation times of breast tissue at 1.5T and 3T measured using IDEAL. J Magn Reson Imaging 2006; 23(1): 87-91. [http://dx.doi.org/10.1002/jmri.20469] [PMID: 16315211]

[20] Butler RS, Chen C, Vashi R, Hooley RJ, Philpotts LE. 3.0 Tesla *vs* 1.5 Tesla breast magnetic resonance imaging in newly diagnosed breast cancer patients. World J Radiol 2013; 5(8): 285-94. [http://dx.doi.org/10.4329/wjr.v5.i8.285] [PMID: 24003354]

[21] Rahbar H, DeMartini WB, Lee AY, Partridge SC, Peacock S, Lehman CD. Accuracy of 3T *versus* 1.5T breast MRI for pre-operative assessment of extent of disease in newly diagnosed DCIS. Eur J Radiol 2015; 84(4): 611-6. [http://dx.doi.org/10.1016/j.ejrad.2014.12.029] [PMID: 25604909]

[22] Lourenco AP, Donegan L, Khalil H, Mainiero MB. Improving outcomes of screening breast MRI with practice evolution: Initial clinical experience with 3T compared to 1.5T. J Magn Reson Imaging 2014; 39(3): 535-9. [http://dx.doi.org/10.1002/jmri.24198] [PMID: 23720144]

[23] Pineda FD, Medved M, Fan X, *et al.* Comparison of dynamic contrast-enhanced MRI parameters of breast lesions at 1.5 and 3.0 T: A pilot study. Br J Radiol 2015; 88(1049): 20150021. [http://dx.doi.org/10.1259/bjr.20150021] [PMID: 25785918]

[24] Uematsu T, Kasami M, Yuen S, Igarashi T, Nasu H. Comparison of 3- and 1.5-T dynamic breast MRI for visualization of spiculated masses previously identified using mammography. AJR Am J Roentgenol 2012; 198(6): W611-7. [http://dx.doi.org/10.2214/AJR.11.7463] [PMID: 22623579]

[25] Ragupathy SKA, Gagliardi T, Redpath TW, *et al.* Comparison of 1.5T and 3T in assessment of suspicious breast lesions. Breast Cancer Res 2010; 12(S3): P18. [http://dx.doi.org/10.1186/bcr2671]

[26] Dietzel M, Wenkel E, Hammon M, *et al.* Does higher field strength translate into better diagnostic accuracy? A prospective comparison of breast MRI at 3 and 1.5 Tesla. Eur J Radiol 2019; 114: 51-6. [http://dx.doi.org/10.1016/j.ejrad.2019.02.033] [PMID: 31005176]

[27] Westra C, Dialani V, Mehta TS, Eisenberg RL. Using T2-weighted sequences to more accurately characterize breast masses seen on MRI. AJR Am J Roentgenol 2014; 202(3): W183-90. [http://dx.doi.org/10.2214/AJR.13.11266] [PMID: 24555613]

[28] Cheon H, Kim HJ, Kim TH, *et al.* Invasive breast cancer: Prognostic value of peritumoral edema identified at preoperative MR imaging. Radiology 2018; 287(1): 68-75. [http://dx.doi.org/10.1148/radiol.2017171157] [PMID: 29315062]

[29] Heiberg EV, Perman WH, Herrmann VM, Janney CG. Dynamic sequential 3D gadolinium-enhanced MRI of the whole breast. Magn Reson Imaging 1996; 14(4): 337-48.

[http://dx.doi.org/10.1016/0730-725X(95)02112-7] [PMID: 8782170]
[30] Flanagan FL, Murray JG, Gilligan P, Stack JP, Ennis JT. Digital subtraction in Gd-DTPA enhanced imaging of the breast. Clin Radiol 1995; 50(12): 848-54. [http://dx.doi.org/10.1016/S0009-9260(05)83106-X] [PMID: 8536396]
[31] Kuhl CK, Schrading S, Strobel K, Schild HH, Hilgers RD, Bieling HB. Abbreviated breast magnetic resonance imaging (MRI): First postcontrast subtracted images and maximum-intensity projection-a novel approach to breast cancer screening with MRI. J Clin Oncol 2014; 32(22): 2304-10. [http://dx.doi.org/10.1200/JCO.2013.52.5386] [PMID: 24958821]
[32] Kuhl CK, Mielcareck P, Klaschik S, *et al.* Dynamic breast MR imaging: Are signal intensity time course data useful for differential diagnosis of enhancing lesions? Radiology 1999; 211(1): 101-10. [http://dx.doi.org/10.1148/radiology.211.1.r99ap38101] [PMID: 10189459]
[33] Marino MA, Helbich T, Baltzer P, Pinker-Domenig K. Multiparametric MRI of the breast: A review. J Magn Reson Imaging 2018; 47(2): 301-15. [http://dx.doi.org/10.1002/jmri.25790] [PMID: 28639300]
[34] Rahbar H, Partridge SC. Multiparametric MR imaging of breast cancer. Magn Reson Imaging Clin N Am 2016; 24(1): 223-38. [http://dx.doi.org/10.1016/j.mric.2015.08.012] [PMID: 26613883]
[35] Helbich TH, Roberts TPL, Gossmann A, *et al.* Quantitative gadopentetate-enhanced MRI of breast tumors: Testing of different analytic methods. Magn Reson Med 2000; 44(6): 915-24. [http://dx.doi.org/10.1002/1522-2594(200012)44:6<915::AID-MRM13>3.0.CO;2-S] [PMID: 11108629]
[36] Mus RD, Borelli C, Bult P, *et al.* Time to enhancement derived from ultrafast breast MRI as a novel parameter to discriminate benign from malignant breast lesions. Eur J Radiol 2017; 89: 90-6. [http://dx.doi.org/10.1016/j.ejrad.2017.01.020] [PMID: 28267555]
[37] Onishi N, Sadinski M, Gibbs P, *et al.* Differentiation between subcentimeter carcinomas and benign lesions using kinetic parameters derived from ultrafast dynamic contrast-enhanced breast MRI. Eur Radiol 2020; 30(2): 756-66. [http://dx.doi.org/10.1007/s00330-019-06392-5] [PMID: 31468162]
[38] Peter SC, Wenkel E, Weiland E, *et al.* Combination of an ultrafast TWIST-VIBE Dixon sequence protocol and diffusion-weighted imaging into an accurate easily applicable classification tool for masses in breast MRI. Eur Radiol 2020; 30(5): 2761-72. [http://dx.doi.org/10.1007/s00330-019-06608-8] [PMID: 32002644]
[39] Shin SU, Cho N, Kim SY, Lee SH, Chang JM, Moon WK. Time-to-enhancement at ultrafast breast DCE-MRI: Potential imaging biomarker of tumour aggressiveness. Eur Radiol 2020; 30(7): 4058-68. [http://dx.doi.org/10.1007/s00330-020-06693-0] [PMID: 32144456]
[40] Kim JJ, Kim JY, Hwangbo L, *et al.* Ultrafast Dynamic Contrast-Enhanced MRI Using Compressed Sensing: Associations of Early Kinetic Parameters With Prognostic Factors of Breast Cancer. AJR Am J Roentgenol 2021; 217(1): 56-63. [http://dx.doi.org/10.2214/AJR.20.23457] [PMID: 33909465]
[41] Lee CS, Moy L. Ultrafast Breast MRI to Predict Pathologic Response after Neoadjuvant Therapy. Radiology 2022; 305(3): 575-7. [http://dx.doi.org/10.1148/radiol.221511] [PMID: 35880985]
[42] Ramtohul T, Tescher C, Vaflard P, *et al.* Prospective evaluation of ultrafast breast MRI for predicting pathologic response after neoadjuvant therapies. Radiology 2022; 305(3): 565-74. [http://dx.doi.org/10.1148/radiol.220389] [PMID: 35880977]
[43] Romeo V. Standardization of Quantitative DCE-MRI Parameters Measurement: An Urgent Need for Breast Cancer Imaging. Acad Radiol 2022; 29(Suppl. 1): S87-8. [http://dx.doi.org/10.1016/j.acra.2021.12.002] [PMID: 34991941]
[44] Mango VL, Morris EA, David Dershaw D, *et al.* Abbreviated protocol for breast MRI: Are multiple sequences needed for cancer detection? Eur J Radiol 2015; 84(1): 65-70. [http://dx.doi.org/10.1016/j.ejrad.2014.10.004] [PMID: 25454099]
[45] Harvey SC, Di Carlo PA, Lee B, Obadina E, Sippo D, Mullen L. An abbreviated protocol for high-risk screening breast MRI saves time and resources. J Am Coll Radiol 2016; 13(11): R74-80. [http://dx.doi.org/10.1016/j.jacr.2016.09.031] [PMID: 27814819]
[46] Oldrini G, Derraz I, Salleron J, Marchal F, Henrot P. Impact of an abbreviated protocol for breast MRI in diagnostic accuracy. Diagn Interv Radiol 2018; 24(1): 12-6. [http://dx.doi.org/10.5152/dir.2018.16609] [PMID: 29317373]
[47] Heacock L, Melsaether AN, Heller SL, *et al.* Evaluation of a known breast cancer using an abbreviated breast MRI protocol: Correlation of imaging characteristics and pathology with lesion detection and conspicuity. Eur J Radiol 2016; 85(4): 815-23. [http://dx.doi.org/10.1016/j.ejrad.2016.01.005] [PMID: 26971429]
[48] Grimm LJ, Soo MS, Yoon S, Kim C, Ghate SV, Johnson KS. Abbreviated screening protocol for breast MRI: A feasibility study. Acad Radiol 2015; 22(9): 1157-62. [http://dx.doi.org/10.1016/j.acra.2015.06.004] [PMID: 26152500]
[49] Moschetta M, Telegrafo M, Rella L, Stabile Ianora AA, Angelelli G. Abbreviated combined MR protocol: A new faster strategy for characterizing breast lesions. Clin Breast Cancer 2016; 16(3): 207-11. [http://dx.doi.org/10.1016/j.clbc.2016.02.008] [PMID: 27108218]
[50] Choi BH, Choi N, Kim MY, Yang JH, Yoo YB, Jung HK. Usefulness of abbreviated breast MRI screening for women with a history of breast cancer surgery. Breast Cancer Res Treat 2018; 167(2): 495-502. [http://dx.doi.org/10.1007/s10549-017-4530-z] [PMID: 29030785]
[51] Kuhl CK. Abbreviated breast MRI for screening women with dense breast: The EA1141 trial. Br J Radiol 2018; 91(1090): 20170441. [http://dx.doi.org/10.1259/bjr.20170441] [PMID: 28749202]
[52] Comstock CE, Gatsonis C, Newstead GM, *et al.* Comparison of Abbreviated Breast MRI *vs* Digital Breast Tomosynthesis for Breast Cancer Detection Among Women With Dense Breasts Undergoing Screening. JAMA 2020; 323(8): 746-56. [http://dx.doi.org/10.1001/jama.2020.0572] [PMID: 32096852]
[53] Onega T, Lee CI, Benkeser D, *et al.* Travel burden to breast MRI and utilization: Are risk and sociodemographics related? J Am Coll Radiol 2016; 13(6): 611-9. [http://dx.doi.org/10.1016/j.jacr.2016.01.022] [PMID: 27026577]
[54] Greenwood HI. Abbreviated protocol breast MRI: The past, present, and future. Clin Imaging 2019; 53: 169-73. [http://dx.doi.org/10.1016/j.clinimag.2018.10.017] [PMID: 30366213]
[55] Pinker K, Helbich TH, Morris EA. The potential of multiparametric MRI of the breast. Br J Radiol 2017; 90(1069): 20160715. [http://dx.doi.org/10.1259/bjr.20160715] [PMID: 27805423]
[56] Zhu CR, Chen KY, Li P, Xia ZY, Wang B. Accuracy of multiparametric MRI in distinguishing the breast malignant lesions from benign lesions: A meta-analysis. Acta Radiol 2021; 62(10): 1290-7. [http://dx.doi.org/10.1177/0284185120963900] [PMID: 33059458]
[57] Le Bihan D, Breton E, Lallemand D, Grenier P, Cabanis E, Laval-Jeantet M. MR imaging of intravoxel incoherent motions: Application to diffusion and perfusion in neurologic disorders. Radiology 1986; 161(2): 401-7. [http://dx.doi.org/10.1148/radiology.161.2.3763909] [PMID: 3763909]
[58] Iima M, Honda M, Sigmund EE, Ohno Kishimoto A, Kataoka M, Togashi K. Diffusion MRI of the breast: Current status and future directions. J Magn Reson Imaging 2020; 52(1): 70-90. [http://dx.doi.org/10.1002/jmri.26908] [PMID: 31520518]
[59] Partridge SC, McDonald ES. Diffusion weighted magnetic resonance imaging of the breast: Protocol optimization, interpretation, and clinical applications. Magn Reson Imaging Clin N Am 2013; 21(3): 601-24. [http://dx.doi.org/10.1016/j.mric.2013.04.007] [PMID: 23928248]
[60] Shi R, Yao Q, Wu L, Xu J. Breast lesions: Diagnosis using diffusion weighted imaging at 1.5T and 3.0T–systematic review and meta-analysis. Clin Breast Cancer 2018; 18(3): e305-20. [http://dx.doi.org/10.1016/j.clbc.2017.06.011] [PMID: 28802529]
[61] Dietzel M, Ellmann S, Schulz-Wendtland R, *et al.* Breast MRI in the era of diffusion weighted imaging: Do we still need signal-intensity time curves? Eur Radiol 2020; 30(1): 47-56. [http://dx.doi.org/10.1007/s00330-019-06346-x] [PMID: 31359125]
[62] Petralia G, Bonello L, Priolo F, Summers P, Bellomi M. Breast MR with special focus on DW-MRI and DCE-MRI. Cancer Imaging 2011; 11(1): 76-90. [http://dx.doi.org/10.1102/1470-7330.2011.0014] [PMID: 21771711]
[63] Newitt DC, Zhang Z, Gibbs JE, *et al.* Test–retest repeatability and reproducibility of ADC measures by breast DWI: Results from the ACRIN 6698 trial. J Magn Reson Imaging 2019; 49(6): 1617-28. [http://dx.doi.org/10.1002/jmri.26539] [PMID: 30350329]
[64] Dorrius MD, Dijkstra H, Oudkerk M, Sijens PE. Effect of b value and pre-admission of contrast on diagnostic accuracy of 1.5-T breast DWI: A systematic review and meta-analysis. Eur Radiol 2014; 24(11): 2835-47. [http://dx.doi.org/10.1007/s00330-014-3338-z] [PMID: 25103535]
[65] Bogner W, Gruber S, Pinker K, *et al.* Diffusion-weighted MR for differentiation of breast lesions at 3.0 T: How does selection of diffusion protocols affect diagnosis? Radiology 2009; 253(2): 341-51. [http://dx.doi.org/10.1148/radiol.2532081718] [PMID: 19703869]

[66] Tamura T, Murakami S, Naito K, Yamada T, Fujimoto T, Kikkawa T. Investigation of the optimal b-value to detect breast tumors with diffusion weighted imaging by 1.5-T MRI. Cancer Imaging 2014; 14(1): 11. [http://dx.doi.org/10.1186/1470-7330-14-11] [PMID: 25608450]

[67] Pereira FPA, Martins G, Figueiredo E, *et al.* Assessment of breast lesions with diffusion-weighted MRI: Comparing the use of different b values. AJR Am J Roentgenol 2009; 193(4): 1030-5. [http://dx.doi.org/10.2214/AJR.09.2522] [PMID: 19770326]

[68] Baxter GC, Graves MJ, Gilbert FJ, Patterson AJ. A Meta-analysis of the Diagnostic Performance of Diffusion MRI for Breast Lesion Characterization. Radiology 2019; 291(3): 632-41. [http://dx.doi.org/10.1148/radiol.2019182510] [PMID: 31012817]

[69] Padhani AR, Liu G, Mu-Koh D, *et al.* Diffusion-weighted magnetic resonance imaging as a cancer biomarker: Consensus and recommendations. Neoplasia 2009; 11(2): 102-25. [http://dx.doi.org/10.1593/neo.81328] [PMID: 19186405]

[70] Iima M, Partridge SC, Le Bihan D. Six DWI questions you always wanted to know but were afraid to ask: Clinical relevance for breast diffusion MRI. Eur Radiol 2020; 30(5): 2561-70. [http://dx.doi.org/10.1007/s00330-019-06648-0] [PMID: 31965256]

[71] Baltzer P, Mann RM, Iima M, *et al.* Diffusion-weighted imaging of the breast—a consensus and mission statement from the EUSOBI International Breast Diffusion-Weighted Imaging working group. Eur Radiol 2020; 30(3): 1436-50. [http://dx.doi.org/10.1007/s00330-019-06510-3] [PMID: 31786616]

[72] Wielema M, Dorrius MD, Pijnappel RM, *et al.* Diagnostic performance of breast tumor tissue selection in diffusion weighted imaging: A systematic review and meta-analysis. PLoS One 2020; 15(5): e0232856. [http://dx.doi.org/10.1371/journal.pone.0232856] [PMID: 32374781]

[73] Wielema M, Sijens PE, Dijkstra H, *et al.* Diffusion weighted imaging of the breast: Performance of standardized breast tumor tissue selection methods in clinical decision making. PLoS One 2021; 16(1): e0245930. [http://dx.doi.org/10.1371/journal.pone.0245930] [PMID: 33493230]

[74] Solomon E, Nissan N, Furman-Haran E, *et al.* Overcoming limitations in diffusion-weighted MRI of breast by spatio-temporal encoding. Magn Reson Med 2015; 73(6): 2163-73. [http://dx.doi.org/10.1002/mrm.25344] [PMID: 25045867]

[75] Pinker K, Moy L, Sutton EJ, *et al.* Diffusion- Weighted imaging with apparent diffusion coefficient mapping for breast cancer detection as a stand-alone parameter: Comparison with dynamic contrast-enhanced and multiparametric magnetic resonance imaging. Invest Radiol 2018; 53(10): 587-95. [http://dx.doi.org/10.1097/RLI.0000000000000465] [PMID: 29620604]

[76] Partridge SC, Nissan N, Rahbar H, Kitsch AE, Sigmund EE. Diffusion-weighted breast MRI: Clinical applications and emerging techniques. J Magn Reson Imaging 2017; 45(2): 337-55. [http://dx.doi.org/10.1002/jmri.25479] [PMID: 27690173]

[77] Barth M, Breuer F, Koopmans PJ, Norris DG, Poser BA. Simultaneous multislice (SMS) imaging techniques. Magn Reson Med 2016; 75(1): 63-81. [http://dx.doi.org/10.1002/mrm.25897] [PMID: 26308571]

[78] Setsompop K, Gagoski BA, Polimeni JR, Witzel T, Wedeen VJ, Wald LL. Blipped-controlled aliasing in parallel imaging for simultaneous multislice echo planar imaging with reduced *g* -factor penalty. Magn Reson Med 2012; 67(5): 1210-24. [http://dx.doi.org/10.1002/mrm.23097] [PMID: 21858868]

[79] Taron J, Martirosian P, Kuestner T, *et al.* Scan time reduction in diffusion-weighted imaging of the pancreas using a simultaneous multislice technique with different acceleration factors: How fast can we go? Eur Radiol 2018; 28(4): 1504-11. [http://dx.doi.org/10.1007/s00330-017-5132-1] [PMID: 29134353]

[80] Barentsz MW, Taviani V, Chang JM, *et al.* Assessment of tumor morphology on diffusion-weighted (DWI) breast MRI: Diagnostic value of reduced field of view DWI. J Magn Reson Imaging 2015; 42(6): 1656-65. [http://dx.doi.org/10.1002/jmri.24929] [PMID: 25914178]

[81] Taviani V, Alley MT, Banerjee S, *et al.* High-resolution diffusion-weighted imaging of the breast with multiband 2D radiofrequency pulses and a generalized parallel imaging reconstruction. Magn Reson Med 2017; 77(1): 209-20. [http://dx.doi.org/10.1002/mrm.26110] [PMID: 26778549]

[82] Park JY, Shin HJ, Shin KC, *et al.* Comparison of readout segmented echo planar imaging (EPI) and EPI with reduced field-of-VIew diffusion-weighted imaging at 3t in patients with breast cancer. J Magn Reson Imaging 2015; 42(6): 1679-88. [http://dx.doi.org/10.1002/jmri.24940] [PMID: 25946597]

[83] Clauser P, Mann R, Athanasiou A, *et al.* A survey by the European Society of Breast Imaging on the utilisation of breast MRI in clinical practice. Eur Radiol 2018; 28(5): 1909-18. [http://dx.doi.org/10.1007/s00330-017-5121-4] [PMID: 29168005]

[84] Iacconi C, Giannelli M, Marini C, *et al.* The role of mean diffusivity (MD) as a predictive index of the response to chemotherapy in locally advanced breast cancer: A preliminary study. Eur Radiol 2010; 20(2): 303-8. [http://dx.doi.org/10.1007/s00330-009-1550-z] [PMID: 19760422]

[85] Park SH, Moon WK, Cho N, *et al.* Diffusion-weighted MR imaging: Pretreatment prediction of response to neoadjuvant chemotherapy in patients with breast cancer. Radiology 2010; 257(1): 56-63. [http://dx.doi.org/10.1148/radiol.10092021] [PMID: 20851939]

[86] Thoeny HC, Ross BD. Predicting and monitoring cancer treatment response with diffusion-weighted MRI. J Magn Reson Imaging 2010; 32(1): 2-16. [http://dx.doi.org/10.1002/jmri.22167] [PMID: 20575076]

[87] Sharma U, Danishad KKA, Seenu V, Jagannathan NR. Longitudinal study of the assessment by MRI and diffusion-weighted imaging of tumor response in patients with locally advanced breast cancer undergoing neoadjuvant chemotherapy. NMR Biomed 2009; 22(1): 104-13. [http://dx.doi.org/10.1002/nbm.1245] [PMID: 18384182]

[88] Pickles MD, Gibbs P, Lowry M, Turnbull LW. Diffusion changes precede size reduction in neoadjuvant treatment of breast cancer. Magn Reson Imaging 2006; 24(7): 843-7. [http://dx.doi.org/10.1016/j.mri.2005.11.005] [PMID: 16916701]

[89] Woodhams R, Kakita S, Hata H, *et al.* Identification of residual breast carcinoma following neoadjuvant chemotherapy: Diffusion-weighted imaging--comparison with contrast-enhanced MR imaging and pathologic findings. Radiology 2010; 254(2): 357-66. [http://dx.doi.org/10.1148/radiol.2542090405] [PMID: 20093508]

[90] D'Orsi CJ, Sickles EA, Mendelson EB, Morris EA. ACR BI- RADS® Atlas, Breast Imaging Reporting and Data System. Reston, VA: American College of Radiology 2013.

[91] Lo Gullo R, Sevilimedu V, Baltzer P, *et al.* A survey by the European Society of Breast Imaging on the implementation of breast diffusion-weighted imaging in clinical practice. Eur Radiol 2022; 32(10): 6588-97. [http://dx.doi.org/10.1007/s00330-022-08833-0] [PMID: 35507050]

[92] Partridge SC, Ziadloo A, Murthy R, *et al.* Diffusion tensor MRI: Preliminary anisotropy measures and mapping of breast tumors. J Magn Reson Imaging 2010; 31(2): 339-47. [http://dx.doi.org/10.1002/jmri.22045] [PMID: 20099346]

[93] Partridge SC, Murthy RS, Ziadloo A, White SW, Allison KH, Lehman CD. Diffusion tensor magnetic resonance imaging of the normal breast. Magn Reson Imaging 2010; 28(3): 320-8. [http://dx.doi.org/10.1016/j.mri.2009.10.003] [PMID: 20061111]

[94] Yamaguchi K, Nakazono T, Egashira R, *et al.* Diagnostic Performance of Diffusion Tensor Imaging with Readout-segmented Echo-planar Imaging for Invasive Breast Cancer: Correlation of ADC and FA with Pathological Prognostic Markers. Magn Reson Med Sci 2017; 16(3): 245-52. [http://dx.doi.org/10.2463/mrms.mp.2016-0037] [PMID: 27853053]

[95] Jiang R, Ma Z, Dong H, Sun S, Zeng X, Li X. Diffusion tensor imaging of breast lesions: Evaluation of apparent diffusion coefficient and fractional anisotropy and tissue cellularity. Br J Radiol 2016; 89(1064): 20160076. [http://dx.doi.org/10.1259/bjr.20160076] [PMID: 27302492]

[96] Baltzer PAT, Schäfer A, Dietzel M, *et al.* Diffusion tensor magnetic resonance imaging of the breast: A pilot study. Eur Radiol 2011; 21(1): 1-10. [http://dx.doi.org/10.1007/s00330-010-1901-9] [PMID: 20668860]

[97] Luo J, Hippe DS, Rahbar H, Parsian S, Rendi MH, Partridge SC. Diffusion tensor imaging for characterizing tumor microstructure and improving diagnostic performance on breast MRI: A prospective observational study. Breast Cancer Res 2019; 21(1): 102. [http://dx.doi.org/10.1186/s13058-019-1183-3] [PMID: 31484577]

[98] Bokacheva L, Kaplan JB, Giri DD, *et al.* Intravoxel incoherent motion diffusion-weighted MRI at 3.0 T differentiates malignant breast lesions from benign lesions and breast parenchyma. J Magn Reson Imaging 2014; 40(4): 813-23. [http://dx.doi.org/10.1002/jmri.24462] [PMID: 24273096]

[99] Cho GY, Moy L, Kim SG, *et al.* Evaluation of breast cancer using

intravoxel incoherent motion (IVIM) histogram analysis: Comparison with malignant status, histological subtype, and molecular prognostic factors. Eur Radiol 2016; 26(8): 2547-58. [http://dx.doi.org/10.1007/s00330-015-4087-3] [PMID: 26615557]

[100] Ma D, Lu F, Zou X, *et al.* Intravoxel incoherent motion diffusion-weighted imaging as an adjunct to dynamic contrast-enhanced MRI to improve accuracy of the differential diagnosis of benign and malignant breast lesions. Magn Reson Imaging 2017; 36: 175-9. [http://dx.doi.org/10.1016/j.mri.2016.10.005] [PMID: 27742437]

[101] Liu C, Liang C, Liu Z, Zhang S, Huang B. Intravoxel incoherent motion (IVIM) in evaluation of breast lesions: Comparison with conventional DWI. Eur J Radiol 2013; 82(12): e782-9. [http://dx.doi.org/10.1016/j.ejrad.2013.08.006] [PMID: 24034833]

[102] Kim Y, Ko K, Kim D, *et al.* Intravoxel incoherent motion diffusion-weighted MR imaging of breast cancer: Association with histopathological features and subtypes. Br J Radiol 2016; 89(1063): 20160140. [http://dx.doi.org/10.1259/bjr.20160140] [PMID: 27197744]

[103] Cho GY, Gennaro L, Sutton EJ, *et al.* Intravoxel incoherent motion (IVIM) histogram biomarkers for prediction of neoadjuvant treatment response in breast cancer patients. Eur J Radiol Open 2017; 4: 101-7. [http://dx.doi.org/10.1016/j.ejro.2017.07.002] [PMID: 28856177]

[104] Iima M. Perfusion-driven Intravoxel Incoherent Motion (IVIM) MRI in Oncology: Applications, Challenges, and Future Trends. Magn Reson Med Sci 2021; 20(2): 125-38. [http://dx.doi.org/10.2463/mrms.rev.2019-0124] [PMID: 32536681]

[105] Le Bihan D. What can we see with IVIM MRI? Neuroimage 2019; 187: 56-67. [http://dx.doi.org/10.1016/j.neuroimage.2017.12.062] [PMID: 29277647]

[106] Iima M, Kataoka M, Kanao S, *et al.* Variability of non-Gaussian diffusion MRI and intravoxel incoherent motion (IVIM) measurements in the breast. PLoS One 2018; 13(3): e0193444. [http://dx.doi.org/10.1371/journal.pone.0193444] [PMID: 29494639]

[107] Le Bihan D, Iima M, Federau C, Sigmund EE. Intravoxel incoherent motion (IVIM) MRI: Principles and applications. Singapore: Jenny Stanford Publishing 2018; pp. 1-533. [http://dx.doi.org/10.1201/9780429427275]

[108] Ichikawa S, Motosugi U, Hernando D, *et al.* Histological grading of hepatocellular carcinomas with intravoxel incoherent motion diffusion-weighted imaging: Inconsistent results depending on the fitting method. Magn Reson Med Sci 2018; 17(2): 168-73. [http://dx.doi.org/10.2463/mrms.mp.2017-0047] [PMID: 28819085]

[109] Nogueira L, Brandao S, Matos E, Nunes RG, Loureiro J, Ramos I, *et al.* Application of the diffusion kurtosis model for the study of breast lesions. Eur Radiol 2014; 24: 1197-203. [http://dx.doi.org/10.1007/s00330-014-3146-5]

[110] Jensen JH, Helpern JA. MRI quantification of non-Gaussian water diffusion by kurtosis analysis. NMR Biomed 2010; 23(7): 698-710. [http://dx.doi.org/10.1002/nbm.1518] [PMID: 20632416]

[111] Tang L, Zhou XJ. Diffusion MRI of cancer: From low to high b-values. J Magn Reson Imaging 2019; 49(1): 23-40. [http://dx.doi.org/10.1002/jmri.26293] [PMID: 30311988]

[112] Li Z, Li X, Peng C, *et al.* The diagnostic performance of diffusion kurtosis imaging in the characterization of breast tumors: A meta-analysis. Front Oncol 2020; 10: 575272. [http://dx.doi.org/10.3389/fonc.2020.575272] [PMID: 33194685]

[113] Liu W, Wei C, Bai J, Gao X, Zhou L. Histogram analysis of diffusion kurtosis imaging in the differentiation of malignant from benign breast lesions. Eur J Radiol 2019; 117: 156-63. [http://dx.doi.org/10.1016/j.ejrad.2019.06.008] [PMID: 31307642]

[114] Palm T, Wenkel E, Ohlmeyer S, *et al.* Diffusion kurtosis imaging does not improve differentiation performance of breast lesions in a short clinical protocol. Magn Reson Imaging 2019; 63: 205-16. [http://dx.doi.org/10.1016/j.mri.2019.08.007] [PMID: 31425816]

[115] Park VY, Kim SG, Kim EK, Moon HJ, Yoon JH, Kim MJ. Diffusional kurtosis imaging for differentiation of additional suspicious lesions on preoperative breast MRI of patients with known breast cancer. Magn Reson Imaging 2019; 62: 199-208. [http://dx.doi.org/10.1016/j.mri.2019.07.011] [PMID: 31323316]

[116] Wu J, Yan F, Chai W, *et al.* Breast cancer recurrence risk prediction using whole-lesion histogram analysis with diffusion kurtosis imaging. Clin Radiol 2020; 75(3): 239.e1-8. [http://dx.doi.org/10.1016/j.crad.2019.10.015] [PMID: 31767139]

[117] Li T, Hong Y, Kong D, Li K. Histogram analysis of diffusion kurtosis imaging based on whole-volume images of breast lesions. J Magn Reson Imaging 2020; 51(2): 627-34. [http://dx.doi.org/10.1002/jmri.26884] [PMID: 31385429]

[118] Borlinhas F, Conceição RC, Ferreira HA. Optimal b-values for diffusion kurtosis imaging in invasive ductal carcinoma *versus* ductal carcinoma *in situ* breast lesions. Australas Phys Eng Sci Med 2019; 42(3): 871-85. [http://dx.doi.org/10.1007/s13246-019-00773-2] [PMID: 31321627]

[119] Huang Y, Lin Y, Hu W, *et al.* Diffusion kurtosis at 3.0T as an *in vivo* imaging marker for breast cancer characterization: Correlation with prognostic factors. J Magn Reson Imaging 2019; 49(3): 845-56. [http://dx.doi.org/10.1002/jmri.26249] [PMID: 30260589]

[120] Jensen JH, Helpern JA, Ramani A, Lu H, Kaczynski K. Diffusional kurtosis imaging: The quantification of non-gaussian water diffusion by means of magnetic resonance imaging. Magn Reson Med 2005; 53(6): 1432-40. [http://dx.doi.org/10.1002/mrm.20508] [PMID: 15906300]

[121] Sun K, Chen X, Chai W, *et al.* Breast cancer: Diffusion kurtosis MR imaging—diagnostic accuracy and correlation with clinical-pathologic factors. Radiology 2015; 277(1): 46-55. [http://dx.doi.org/10.1148/radiol.15141625] [PMID: 25938679]

[122] Bolan PJ, Nelson MT, Yee D, Garwood M. Imaging in breast cancer: Magnetic resonance spectroscopy. Breast Cancer Res 2005; 7(4): 149-52. [http://dx.doi.org/10.1186/bcr1202] [PMID: 15987466]

[123] Bolan PJ. Magnetic resonance spectroscopy of the breast: Current status. Magn Reson Imaging Clin N Am 2013; 21(3): 625-39. [http://dx.doi.org/10.1016/j.mric.2013.04.008] [PMID: 23928249]

[124] Hanahan D, Weinberg RA. Hallmarks of cancer: The next generation. Cell 2011; 144(5): 646-74. [http://dx.doi.org/10.1016/j.cell.2011.02.013] [PMID: 21376230]

[125] Bartella L, Huang W. Proton (1H) MR spectroscopy of the breast. Radiographics 2007; 27(Suppl. 1): S241-52. [http://dx.doi.org/10.1148/rg.27si075504] [PMID: 18180230]

[126] Pinker K, Stadlbauer A, Bogner W, Gruber S, Helbich TH. Molecular imaging of cancer: MR spectroscopy and beyond. Eur J Radiol 2012; 81(3): 566-77. [http://dx.doi.org/10.1016/j.ejrad.2010.04.028] [PMID: 20554145]

[127] Sardanelli F, Fausto A, Podo F. MR spectroscopy of the breast. Radiol Med (Torino) 2008; 113(1): 56-64. [http://dx.doi.org/10.1007/s11547-008-0228-y] [PMID: 18338127]

[128] Baltzer PAT, Dietzel M. Breast lesions: Diagnosis by using proton MR spectroscopy at 1.5 and 3.0 T--systematic review and meta-analysis. Radiology 2013; 267(3): 735-46. [http://dx.doi.org/10.1148/radiol.13121856] [PMID: 23468577]

[129] Montemezzi S, Cavedon C, Camera L, *et al.* ^{1}H-MR spectroscopy of suspicious breast mass lesions at 3T: A clinical experience. Radiol Med (Torino) 2017; 122(3): 161-70. [http://dx.doi.org/10.1007/s11547-016-0713-7] [PMID: 27981485]

[130] Jagannathan NR, Kumar M, Seenu V, *et al.* Evaluation of total choline from in-vivo volume localized proton MR spectroscopy and its response to neoadjuvant chemotherapy in locally advanced breast cancer. Br J Cancer 2001; 84(8): 1016-22. [http://dx.doi.org/10.1054/bjoc.2000.1711] [PMID: 11308247]

[131] Meisamy S, Bolan PJ, Baker EH, *et al.* Neoadjuvant chemotherapy of locally advanced breast cancer: Predicting response with *in vivo* (1)H MR spectroscopy--a pilot study at 4 T. Radiology 2004; 233(2): 424-31. [http://dx.doi.org/10.1148/radiol.2332031285] [PMID: 15516615]

[132] Bolan PJ, Kim E, Herman BA, *et al.* MR spectroscopy of breast cancer for assessing early treatment response: Results from the ACRIN 6657 MRS trial. J Magn Reson Imaging 2017; 46(1): 290-302. [http://dx.doi.org/10.1002/jmri.25560] [PMID: 27981651]

[133] Fardanesh R, Marino MA, Avendano D, Leithner D, Pinker K, Thakur SB. Proton MR spectroscopy in the breast: Technical innovations and clinical applications. J Magn Reson Imaging 2019; 50(4): 1033-46. [http://dx.doi.org/10.1002/jmri.26700] [PMID: 30848037]

[134] Thakur SB, Brennan SB, Ishill NM, *et al.* Diagnostic usefulness of water-to-fat ratio and choline concentration in malignant and benign breast lesions and normal breast parenchyma: An *in vivo*^{1} H MRS study. J Magn Reson Imaging 2011; 33(4): 855-63. [http://dx.doi.org/10.1002/jmri.22493] [PMID: 21448950]

[135] Thakur SB, Horvat JV, Hancu I, *et al.* Quantitative *in vivo* proton MR spectroscopic assessment of lipid metabolism: Value for breast cancer diagnosis and prognosis. J Magn Reson Imaging 2019; 50(1): 239-49. [http://dx.doi.org/10.1002/jmri.26622]

[136] Kaggie JD, Hadley JR, Badal J, *et al.* A 3 T sodium and proton composite array breast coil. Magn Reson Med 2014; 71(6): 2231-42. [http://dx.doi.org/10.1002/mrm.24860] [PMID: 24105740]

[137] Ouwerkerk R, Jacobs MA, Macura KJ, *et al.* Elevated tissue sodium concentration in malignant breast lesions detected with non-invasive ^{23}Na MRI. Breast Cancer Res Treat 2007; 106(2): 151-60. [http://dx.doi.org/10.1007/s10549-006-9485-4] [PMID: 17260093]

[138] Zaric O, Pinker K, Zbyn S, *et al.* Quantitative sodium mr imaging at 7 T: Initial results and comparison with diffusion-weighted imaging in patients with breast tumors. Radiology 2016; 280(1): 39-48. [http://dx.doi.org/10.1148/radiol.2016151304] [PMID: 27007803]

[139] Podo F. Tumour phospholipid metabolism. NMR Biomed 1999; 12(7): 413-39. [http://dx.doi.org/10.1002/(SICI)1099-1492(199911)12:7<413::AID-NBM587>3.0.CO;2-U] [PMID: 10654290]

[140] Klomp DWJ, van de Bank BL, Raaijmakers A, *et al.* ^{31} P MRSI and ^{1} H MRS at 7 T: Initial results in human breast cancer. NMR Biomed 2011; 24(10): 1337-42. [http://dx.doi.org/10.1002/nbm.1696] [PMID: 21433156]

[141] Wijnen JP, van der Kemp WJM, Luttje MP, Korteweg MA, Luijten PR, Klomp DWJ. Quantitative ^{31} P magnetic resonance spectroscopy of the human breast at 7 T. Magn Reson Med 2012; 68(2): 339-48. [http://dx.doi.org/10.1002/mrm.23249] [PMID: 22213214]

[142] Schmitt B, Trattnig S, Schlemmer HP. CEST-imaging: A new contrast in MR-mammography by means of chemical exchange saturation transfer. Eur J Radiol 2012; 81(Suppl. 1): S144-6. [http://dx.doi.org/10.1016/S0720-048X(12)70060-8] [PMID: 23083567]

[143] Schmitt B, Zamecnik P, Zaiß M, *et al.* A new contrast in MR mammography by means of chemical exchange saturation transfer (CEST) imaging at 3 Tesla: Preliminary results. Röfo Fortschr Geb Röntgenstr Neuen Bildgeb Verfahr 2011; 183(11): 1030-6. [http://dx.doi.org/10.1055/s-0031-1281764] [PMID: 22034086]

[144] Nasrallah FA, Pagès G, Kuchel PW, Golay X, Chuang KH. Imaging brain deoxyglucose uptake and metabolism by glucoCEST MRI. J Cereb Blood Flow Metab 2013; 33(8): 1270-8. [http://dx.doi.org/10.1038/jcbfm.2013.79] [PMID: 23673434]

[145] Ruan K, Song G, Ouyang G. Role of hypoxia in the hallmarks of human cancer. J Cell Biochem 2009; 107(6): 1053-62. [http://dx.doi.org/10.1002/jcb.22214] [PMID: 19479945]

[146] O'Flynn EAM, deSouza NM. Functional magnetic resonance: Biomarkers of response in breast cancer. Breast Cancer Res 2011; 13(1): 204. [http://dx.doi.org/10.1186/bcr2815] [PMID: 21392409]

[147] Rakow-Penner R, Daniel B, Glover GH. Detecting blood oxygen level-dependent (BOLD) contrast in the breast. J Magn Reson Imaging 2010; 32(1): 120-9. [http://dx.doi.org/10.1002/jmri.22227] [PMID: 20578018]

[148] Brindle KM, Bohndiek SE, Gallagher FA, Kettunen MI. Tumor imaging using hyperpolarized ^{13} C magnetic resonance spectroscopy. Magn Reson Med 2011; 66(2): 505-19. [http://dx.doi.org/10.1002/mrm.22999] [PMID: 21661043]

[149] Albers MJ, Bok R, Chen AP, *et al.* Hyperpolarized 13C lactate, pyruvate, and alanine: Noninvasive biomarkers for prostate cancer detection and grading. Cancer Res 2008; 68(20): 8607-15. [http://dx.doi.org/10.1158/0008-5472.CAN-08-0749] [PMID: 18922937]

[150] Asghar Butt S, Søgaard LV, Ardenkjaer-Larsen JH, *et al.* Monitoring mammary tumor progression and effect of tamoxifen treatment in MMTV-PymT using MRI and magnetic resonance spectroscopy with hyperpolarized [1- ^{13} C]pyruvate. Magn Reson Med 2015; 73(1): 51-8. [http://dx.doi.org/10.1002/mrm.25095] [PMID: 24435823]

[151] Deike-Hofmann K, Koenig F, Paech D, *et al.* Abbreviated MRI Protocols in Breast Cancer Diagnostics. J Magn Reson Imaging 2019; 49(3): 647-58. [http://dx.doi.org/10.1002/jmri.26525] [PMID: 30328180]

[152] Heller SL, Moy L. MRI breast screening revisited. J Magn Reson Imaging 2019; 49(5): 1212-21. [http://dx.doi.org/10.1002/jmri.26547] [PMID: 30693603]

[153] Baltzer PAT, Bickel H, Spick C, *et al.* Potential of noncontrast magnetic resonance imaging with diffusion-weighted imaging in characterization of breast lesions: Intraindividual comparison with dynamic contrast- enhanced magnetic resonance imaging. Invest Radiol 2018; 53(4): 229-35. [http://dx.doi.org/10.1097/RLI.0000000000000433] [PMID: 29190227]

[154] McDonald ES, Hammersley JA, Chou SHS, *et al.* Performance of DWI as a rapid unenhanced technique for detecting mammographically occult breast cancer in elevated-risk women with dense breasts. AJR Am J Roentgenol 2016; 207(1): 205-16. [http://dx.doi.org/10.2214/AJR.15.15873] [PMID: 27077731]

[155] Bu Y, Xia J, Joseph B, *et al.* Non-contrast MRI for breast screening: Preliminary study on detectability of benign and malignant lesions in women with dense breasts. Breast Cancer Res Treat 2019; 177(3): 629-39. [http://dx.doi.org/10.1007/s10549-019-05342-5] [PMID: 31325074]

[156] Liao GJ, Henze Bancroft LC, Strigel RM, *et al.* Background parenchymal enhancement on breast MRI: A comprehensive review. J Magn Reson Imaging 2020; 51(1): 43-61. [http://dx.doi.org/10.1002/jmri.26762] [PMID: 31004391]

[157] Morris EA, Comstock CE, Lee CH, *et al.* ACR BI-RADS® Magnetic Resonance Imaging.ACR BI-RADS® Atlas, Breast Imaging Reporting and Data System. Reston, VA: American College of Radiology 2013.

[158] Jansen SA, Shimauchi A, Zak L, Fan X, Karczmar GS, Newstead GM. The diverse pathology and kinetics of mass, nonmass, and focus enhancement on MR imaging of the breast. J Magn Reson Imaging 2011; 33(6): 1382-9. [http://dx.doi.org/10.1002/jmri.22567] [PMID: 21591007]

[159] Gutierrez RL, DeMartini WB, Eby PR, Kurland BF, Peacock S, Lehman CD. BI-RADS lesion characteristics predict likelihood of malignancy in breast MRI for masses but not for nonmasslike enhancement. AJR Am J Roentgenol 2009; 193(4): 994-1000. [http://dx.doi.org/10.2214/AJR.08.1983] [PMID: 19770321]

[160] Sung JS, Jochelson MS, Brennan S, *et al.* MR imaging features of triple-negative breast cancers. Breast J 2013; 19(6): 643-9. [http://dx.doi.org/10.1111/tbj.12182] [PMID: 24015869]

[161] Bitencourt AGV, Graziano L, Osório CABT, *et al.* MRI Features of Mucinous Cancer of the Breast: Correlation With Pathologic Findings and Other Imaging Methods. AJR Am J Roentgenol 2016; 206(2): 238-46. [http://dx.doi.org/10.2214/AJR.15.14851] [PMID: 26797349]

[162] Chikarmane SA, Michaels AY, Giess CS. Revisiting nonmass enhancement in breast MRI: Analysis of outcomes and follow-up using the updated BI-RADS atlas. AJR Am J Roentgenol 2017; 209(5): 1178-84. [http://dx.doi.org/10.2214/AJR.17.18086] [PMID: 28834447]

[163] Aydin H. The MRI characteristics of non-mass enhancement lesions of the breast: Associations with malignancy. Br J Radiol 2019; 92(1096): 20180464. [http://dx.doi.org/10.1259/bjr.20180464] [PMID: 30673299]

[164] Dietzel M, Baltzer PAT. How to use the Kaiser score as a clinical decision rule for diagnosis in multiparametric breast MRI: A pictorial essay. Insights Imaging 2018; 9(3): 325-35. [http://dx.doi.org/10.1007/s13244-018-0611-8] [PMID: 29616496]

[165] Marino MA, Clauser P, Woitek R, *et al.* A simple scoring system for breast MRI interpretation: Does it compensate for reader experience? Eur Radiol 2016; 26(8): 2529-37. [http://dx.doi.org/10.1007/s00330-015-4075-7] [PMID: 26511631]

[166] Baltzer PAT, Dietzel M, Kaiser WA. A simple and robust classification tree for differentiation between benign and malignant lesions in MR-mammography. Eur Radiol 2013; 23(8): 2051-60. [http://dx.doi.org/10.1007/s00330-013-2804-3] [PMID: 23579418]

[167] Milos RI, Pipan F, Kalovidouri A, *et al.* The Kaiser score reliably excludes malignancy in benign contrast-enhancing lesions classified as BI-RADS 4 on breast MRI high-risk screening exams. Eur Radiol 2020; 30(11): 6052-61. [http://dx.doi.org/10.1007/s00330-020-06945-z] [PMID: 32504098]

[168] Houser M, Barreto D, Mehta A, Brem RF. Current and Future Directions of Breast MRI. J Clin Med 2021; 10(23): 5668. [http://dx.doi.org/10.3390/jcm10235668] [PMID: 34884370]

[169] Lee JM, Abraham L, Lam DL, *et al.* Cumulative risk distribution for interval invasive second breast cancers after negative surveillance mammography. J Clin Oncol 2018; 36(20): 2070-7. [http://dx.doi.org/10.1200/JCO.2017.76.8267] [PMID: 29718790]

[170] Yoo EY, Nam SY, Choi HY, Hong MJ. Agreement between MRI and pathologic analyses for determination of tumor size and correlation with immunohistochemical factors of invasive breast carcinoma. Acta Radiol 2018; 59(1): 50-7. [http://dx.doi.org/10.1177/0284185117705010] [PMID: 28425758]

[171] Mann RM, Hoogeveen YL, Blickman JG, Boetes C. MRI compared to conventional diagnostic work-up in the detection and evaluation of invasive lobular carcinoma of the breast: A review of existing literature. Breast Cancer Res Treat 2008; 107(1): 1-14. [http://dx.doi.org/10.1007/s10549-007-9528-5] [PMID: 18043894]

[172] Karlsson A, Gonzalez V, Jaraj SJ, *et al.* The accuracy of incremental pre-operative breast MRI findings – Concordance with histopathology in the Swedish randomized multicenter POMB trial. Eur J Radiol

2019; 114: 185-91.
[http://dx.doi.org/10.1016/j.ejrad.2019.03.005] [PMID: 31005171]

[173] Houssami N, Ciatto S, Macaskill P, *et al.* Accuracy and surgical impact of magnetic resonance imaging in breast cancer staging: Systematic review and meta-analysis in detection of multifocal and multicentric cancer. J Clin Oncol 2008; 26(19): 3248-58.
[http://dx.doi.org/10.1200/JCO.2007.15.2108] [PMID: 18474876]

[174] Houssami N, Turner RM, Morrow M. Meta-analysis of pre-operative magnetic resonance imaging (MRI) and surgical treatment for breast cancer. Breast Cancer Res Treat 2017; 165(2): 273-83.
[http://dx.doi.org/10.1007/s10549-017-4324-3] [PMID: 28589366]

[175] Sardanelli F, Trimboli RM, Houssami N, *et al.* Solving the preoperative breast MRI conundrum: Design and protocol of the MIPA study. Eur Radiol 2020; 30(10): 5427-36.
[http://dx.doi.org/10.1007/s00330-020-06824-7] [PMID: 32377813]

[176] Sardanelli F, Trimboli RM, Houssami N, *et al.* Magnetic resonance imaging before breast cancer surgery: Results of an observational multicenter international prospective analysis (MIPA). Eur Radiol 2022; 32(3): 1611-23. Epub ahead of print
[PMID: 34643778]

[177] Saslow D, Boetes C, Burke W, *et al.* American Cancer Society guidelines for breast screening with MRI as an adjunct to mammography. CA Cancer J Clin 2007; 57(2): 75-89.
[http://dx.doi.org/10.3322/canjclin.57.2.75] [PMID: 17392385]

[178] Monticciolo DL, Newell MS, Moy L, Niell B, Monsees B, Sickles EA. Breast cancer screening in women at higher-than-average risk: recommendations from the ACR. J Am Coll Radiol 2018; 15(3,3 Pt A): 408-14.

[179] Kriege M, Brekelmans CTM, Boetes C, *et al.* Efficacy of MRI and mammography for breast-cancer screening in women with a familial or genetic predisposition. N Engl J Med 2004; 351(5): 427-37.
[http://dx.doi.org/10.1056/NEJMoa031759] [PMID: 15282350]

[180] Lo G, Scaranelo AM, Aboras H, *et al.* Evaluation of the Utility of Screening Mammography for High-Risk Women Undergoing Screening Breast MR Imaging. Radiology 2017; 285(1): 36-43.
[http://dx.doi.org/10.1148/radiol.2017161103] [PMID: 28586291]

[181] Sippo DA, Burk KS, Mercaldo SF, *et al.* Performance of Screening Breast MRI across Women with Different Elevated Breast Cancer Risk Indications. Radiology 2019; 292(1): 51-9.
[http://dx.doi.org/10.1148/radiol.2019181136] [PMID: 31063080]

[182] Tieu MT, Cigsar C, Ahmed S, *et al.* Breast cancer detection among young survivors of pediatric Hodgkin lymphoma with screening magnetic resonance imaging. Cancer 2014; 120(16): 2507-13.
[http://dx.doi.org/10.1002/cncr.28747] [PMID: 24888639]

[183] Freitas V, Scaranelo A, Menezes R, Kulkarni S, Hodgson D, Crystal P. Added cancer yield of breast magnetic resonance imaging screening in women with a prior history of chest radiation therapy. Cancer 2013; 119(3): 495-503.
[http://dx.doi.org/10.1002/cncr.27771] [PMID: 22952042]

[184] Phi XA, Saadatmand S, De Bock GH, *et al.* Contribution of mammography to MRI screening in BRCA mutation carriers by BRCA status and age: Individual patient data meta-analysis. Br J Cancer 2016; 114(6): 631-7.
[http://dx.doi.org/10.1038/bjc.2016.32] [PMID: 26908327]

[185] Vreemann S, van Zelst JCM, Schlooz-Vries M, *et al.* The added value of mammography in different age-groups of women with and without BRCA mutation screened with breast MRI. Breast Cancer Res 2018; 20(1): 84.
[http://dx.doi.org/10.1186/s13058-018-1019-6] [PMID: 30075794]

[186] Obdeijn IM, Winter-Warnars GAO, Mann RM, Hooning MJ, Hunink MGM, Tilanus-Linthorst MMA. Should we screen BRCA1 mutation carriers only with MRI? A multicenter study. Breast Cancer Res Treat 2014; 144(3): 577-82.
[http://dx.doi.org/10.1007/s10549-014-2888-8] [PMID: 24567197]

[187] Bahl M. Screening MRI in women at intermediate breast cancer risk: An update of the recent literature. J Breast Imaging 2022; 4(3): 231-40.
[http://dx.doi.org/10.1093/jbi/wbac021] [PMID: 35783682]

[188] Port ER, Park A, Borgen PI, Morris E, Montgomery LL. Results of MRI screening for breast cancer in high-risk patients with LCIS and atypical hyperplasia. Ann Surg Oncol 2007; 14(3): 1051-7.
[http://dx.doi.org/10.1245/s10434-006-9195-5] [PMID: 17206485]

[189] Sung JS, Malak SF, Bajaj P, Alis R, Dershaw DD, Morris EA. Screening breast MR imaging in women with a history of lobular carcinoma *in situ*. Radiology 2011; 261(2): 414-20.
[http://dx.doi.org/10.1148/radiol.11110091] [PMID: 21900617]

[190] Chikarmane SA, Giess CS. Screening breast MRI in patients with history of atypia or lobular neoplasia. Breast J 2019; 25(3): 484-7.
[http://dx.doi.org/10.1111/tbj.13259] [PMID: 30972867]

[191] Park VY, Kim MJ, Kim GR, Yoon JH. Outcomes following neg- ative screening MRI results in Korean women with a personal history of breast cancer: Implications for the next MRI interval. Radiology 2021; 300(2): 303-11.
[http://dx.doi.org/10.1148/radiol.2021204217] [PMID: 34032514]

[192] Strigel RM, Rollenhagen J, Burnside ES, *et al.* Screening breast MRI outcomes in routine clinical practice: Comparison to BI-RADS benchmarks. Acad Radiol 2017; 24(4): 411-7.
[http://dx.doi.org/10.1016/j.acra.2016.10.014] [PMID: 27986508]

[193] Tadros A, Arditi B, Weltz C, Port E, Margolies LR, Schmidt H. Utility of surveillance MRI in women with a personal history of breast cancer. Clin Imaging 2017; 46: 33-6.
[http://dx.doi.org/10.1016/j.clinimag.2017.06.007] [PMID: 28700966]

[194] Liu H, Hua Y, Peng W, Zhang X. Surveillance magnetic reso- nance imaging in detecting the second breast cancer in women with a personal history of breast cancer. J Comput Assist Tomogr 2019; 43(6): 937-42.
[http://dx.doi.org/10.1097/RCT.0000000000000931] [PMID: 31738203]

[195] Li T, Sun L, Miller N, *et al.* The association of measured breast tissue characteristics with mammographic density and other risk factors for breast cancer. Cancer Epidemiol Biomarkers Prev 2005; 14(2): 343-9.
[http://dx.doi.org/10.1158/1055-9965.EPI-04-0490] [PMID: 15734956]

[196] Hawes D, Downey S, Pearce CL, *et al.* Dense breast stromal tissue shows greatly increased concentration of breast epithelium but no increase in its proliferative activity 2006.
[http://dx.doi.org/10.1186/bcr1408]

[197] Alowami S, Troup S, Al-Haddad S, Kirkpatrick I, Watson PH. Mammographic density is related to stroma and stromal proteoglycan expression. Breast Cancer Res 2003; 5(5): R129-35.
[http://dx.doi.org/10.1186/bcr622] [PMID: 12927043]

[198] Carney PA, Miglioretti DL, Yankaskas BC, *et al.* Individual and combined effects of age, breast density, and hormone replacement therapy use on the accuracy of screening mammography. Ann Intern Med 2003; 138(3): 168-75.
[http://dx.doi.org/10.7326/0003-4819-138-3-200302040-00008] [PMID: 12558355]

[199] Boyd NF, Guo H, Martin LJ, *et al.* Mammographic density and the risk and detection of breast cancer. N Engl J Med 2007; 356(3): 227-36.
[http://dx.doi.org/10.1056/NEJMoa062790] [PMID: 17229950]

[200] Mandelson MT, Oestreicher N, Porter PL, *et al.* Breast density as a predictor of mammographic detection: Comparison of interval- and screen-detected cancers. J Natl Cancer Inst 2000; 92(13): 1081-7.
[http://dx.doi.org/10.1093/jnci/92.13.1081] [PMID: 10880551]

[201] Fletcher SW, Elmore JG. Clinical practice. Mammographic screening for breast cancer. N Engl J Med 2003; 348(17): 1672-80.
[http://dx.doi.org/10.1056/NEJMcp021804] [PMID: 12711743]

[202] Wolfe JN. Risk for breast cancer development determined by mammographic parenchymal pattern Cancer 1976; 37(2): 2486-92.

[203] Wolfe JN. Breast patterns as an index of risk for developing breast cancer. AJR Am J Roentgenol 1976; 126(6): 1130-7.
[http://dx.doi.org/10.2214/ajr.126.6.1130] [PMID: 179369]

[204] McCormack VA, dos Santos Silva I. Breast density and parenchymal patterns as markers of breast cancer risk: A meta-analysis. Cancer Epidemiol Biomarkers Prev 2006; 15(6): 1159-69.
[http://dx.doi.org/10.1158/1055-9965.EPI-06-0034] [PMID: 16775176]

[205] Boyd NF, Byng JW, Jong RA, *et al.* Quantitative classification of mammographic densities and breast cancer risk: Results from the Canadian National Breast Screening Study. J Natl Cancer Inst 1995; 87(9): 670-5.
[http://dx.doi.org/10.1093/jnci/87.9.670] [PMID: 7752271]

[206] Melnikow J, Fenton JJ, Whitlock EP, *et al.* Supplemental screening for breast cancer in women with dense breasts: A systematic review for the U.S. preventive services task force. Ann Intern Med 2016; 164(4): 268-78.
[http://dx.doi.org/10.7326/M15-1789] [PMID: 26757021]

[207] Zhang Z, Zhang Z, Lehrer D, *et al.* Detection of breast cancer with addition of annual screening ultrasound or a single screening MRI to mammography in women with elevated breast cancer risk. JAMA 2012; 307(13): 1394-404.
[http://dx.doi.org/10.1001/jama.2012.388] [PMID: 22474203]

[208] Ratushnyak S, Hoogendoorn M, van Baal PHM. Cost-effectiveness of

cancer screening: Health and costs in life years gained. Am J Prev Med 2019; 57(6): 792-9.
[http://dx.doi.org/10.1016/j.amepre.2019.07.027] [PMID: 31753260]

[209] Geuzinge HA, Bakker MF, Heijnsdijk EAM, *et al.* Cost- effectiveness of MRI screening for women with extremely dense breast tissue. J Natl Cancer Inst 2021; 113(11): 1476-83.
[http://dx.doi.org/10.1093/jnci/djab119] [PMID: 34585249]

[210] Mann RM, Athanasiou A, Baltzer PAT, *et al.* Breast cancer screening in women with extremely dense breasts recommendations of the European Society of Breast Imaging (EUSOBI). Eur Radiol 2022; 32(6): 4036-45.
[http://dx.doi.org/10.1007/s00330-022-08617-6] [PMID: 35258677]

[211] Marinovich ML, Houssami N, Macaskill P, *et al.* Meta-analysis of magnetic resonance imaging in detecting residual breast cancer after neoadjuvant therapy. J Natl Cancer Inst 2013; 105(5): 321-33.
[http://dx.doi.org/10.1093/jnci/djs528] [PMID: 23297042]

[212] Scheel JR, Kim E, Partridge SC, *et al.* MRI, clinical examination, and mammography for preoperative assessment of residual disease and pathologic complete response after neoadjuvant chemotherapy for breast cancer: ACRIN 6657 trial. AJR Am J Roentgenol 2018; 210(6): 1376-85.
[http://dx.doi.org/10.2214/AJR.17.18323] [PMID: 29708782]

[213] Croshaw R, Shapiro-Wright H, Svensson E, Erb K, Julian T. Accuracy of clinical examination, digital mammogram, ultrasound, and MRI in determining postneoadjuvant pathologic tumor response in operable breast cancer patients. Ann Surg Oncol 2011; 18(11): 3160-3.
[http://dx.doi.org/10.1245/s10434-011-1919-5] [PMID: 21947594]

[214] Sheikhbahaei S, Trahan TJ, Xiao J, *et al.* FDG-PET/CT and MRI for Evaluation of Pathologic Response to Neoadjuvant Chemotherapy in Patients With Breast Cancer: A Meta-Analysis of Diagnostic Accuracy Studies. Oncologist 2016; 21(8): 931-9.
[http://dx.doi.org/10.1634/theoncologist.2015-0353] [PMID: 27401897]

[215] Mukhtar RA, Yau C, Rosen M, Tandon VJ, Hylton N, Esserman LJ. Clinically meaningful tumor reduction rates vary by prechemotherapy MRI phenotype and tumor subtype in the I-SPY 1 TRIAL (CALGB 150007/150012; ACRIN 6657). Ann Surg Oncol 2013; 20(12): 3823-30.
[http://dx.doi.org/10.1245/s10434-013-3038-y] [PMID: 23780381]

[216] Negrão EMS, Souza JA, Marques EF, Bitencourt AGV. Breast cancer phenotype influences MRI response evaluation after neoadjuvant chemotherapy. Eur J Radiol 2019; 120: 108701.
[http://dx.doi.org/10.1016/j.ejrad.2019.108701] [PMID: 31610321]

[217] Denis F, Desbiez-Bourcier AV, Chapiron C, Arbion F, Body G, Brunereau L. Contrast enhanced magnetic resonance imaging underestimates residual disease following neoadjuvant docetaxel based chemotherapy for breast cancer. Eur J Surg Oncol 2004; 30(10): 1069-76.
[http://dx.doi.org/10.1016/j.ejso.2004.07.024] [PMID: 15522553]

[218] Schrading S, Kuhl CK. Breast Cancer: Influence of Taxanes on Response Assessment with Dynamic Contrast-enhanced MR Imaging. Radiology 2015; 277(3): 687-96.
[http://dx.doi.org/10.1148/radiol.2015150006] [PMID: 26176656]

[219] Chen JH, Bahri S, Mehta RS, *et al.* Impact of factors affecting the residual tumor size diagnosed by MRI following neoadjuvant chemotherapy in comparison to pathology. J Surg Oncol 2014; 109(2): 158-67.
[http://dx.doi.org/10.1002/jso.23470] [PMID: 24166728]

[220] Reig B, Lewin AA, Du L, *et al.* Breast MRI for Evaluation of Response to Neoadjuvant Therapy. Radiographics 2021; 41(3): 665-79.
[http://dx.doi.org/10.1148/rg.2021200134] [PMID: 33939542]

[221] Eisenhauer EA, Therasse P, Bogaerts J, *et al.* New response evaluation criteria in solid tumours: Revised RECIST guideline (version 1.1). Eur J Cancer 2009; 45(2): 228-47.
[http://dx.doi.org/10.1016/j.ejca.2008.10.026] [PMID: 19097774]

[222] Ah-See MLW, Makris A, Taylor NJ, *et al.* Early changes in functional dynamic magnetic resonance imaging predict for pathologic response to neoadjuvant chemotherapy in primary breast cancer. Clin Cancer Res 2008; 14(20): 6580-9.
[http://dx.doi.org/10.1158/1078-0432.CCR-07-4310] [PMID: 18927299]

[223] Dogan BE, Yuan Q, Bassett R, *et al.* Comparing the performances of magnetic resonance imaging size *vs* pharmacokinetic parameters to predict response to neoadjuvant chemotherapy and survival in patients with breast cancer. Curr Probl Diagn Radiol 2019; 48(3): 235-40.
[http://dx.doi.org/10.1067/j.cpradiol.2018.03.003] [PMID: 29685400]

[224] Partridge SC, Zhang Z, Newitt DC, *et al.* Diffusion-weighted MRI findings predict pathologic response in neoadjuvant treatment of breast cancer: The ACRIN 6698 Multicenter Trial. Radiology 2018; 289(3): 618-27.
[http://dx.doi.org/10.1148/radiol.2018180273] [PMID: 30179110]

[225] Chu W, Jin W, Liu D, *et al.* Diffusion-weighted imaging in identifying breast cancer pathological response to neoadjuvant chemotherapy: A meta-analysis. Oncotarget 2018; 9(6): 7088-100.
[http://dx.doi.org/10.18632/oncotarget.23195] [PMID: 29467952]

[226] Santamaría G, Bargalló X, Fernández PL, Farrús B, Caparrós X, Velasco M. Neoadjuvant systemic therapy in breast cancer: Association of contrast-enhanced MR imaging findings, diffusion-weighted imaging findings, and tumor subtype with tumor response. Radiology 2017; 283(3): 663-72.
[http://dx.doi.org/10.1148/radiol.2016160176] [PMID: 27875106]

[227] Kim SY, Cho N, Shin SU, *et al.* Contrast-enhanced MRI after neoadjuvant chemotherapy of breast cancer: Lesion-to-background parenchymal signal enhancement ratio for discriminating pathological complete response from minimal residual tumour. Eur Radiol 2018; 28(7): 2986-95.
[http://dx.doi.org/10.1007/s00330-017-5251-8] [PMID: 29380033]

[228] Ofri A, Moore K. Occult breast cancer: Where are we at? Breast 2020; 54: 211-5.
[http://dx.doi.org/10.1016/j.breast.2020.10.012] [PMID: 33130487]

[229] Hessler LK, *et al.* Factors influencing management and outcome in patients with occult breast cancer with axillary lymph node involvement: Analysis of the national cancer database 2017.
[http://dx.doi.org/10.1245/s10434-017-5928-x]

[230] de Bresser J, *et al.* Breast MRI in clinically and mammographically occult breast cancer presenting with an axillary metastasis: A systematic review 2010.
[http://dx.doi.org/10.1016/j.ejso.2009.09.007]

[231] Galimberti V, Bassani G, Monti S, *et al.* Clinical experience with axillary presentation breast cancer. Breast Cancer Res Treat 2004; 88(1): 43-7.
[http://dx.doi.org/10.1007/s10549-004-9453-9] [PMID: 15538044]

[232] Bennani-Baiti B, Bennani-Baiti N, Baltzer PA. Diagnostic performance of breast magnetic resonance imaging in non-calcified equivocal breast findings: Results from a systematic review and meta-analysis. PLoS One 2016; 11(8): e0160346.
[http://dx.doi.org/10.1371/journal.pone.0160346] [PMID: 27482715]

[233] Bennani-Baiti B, Baltzer PA. MR imaging for diagnosis of malignancy in mammographic microcalcifications: A systematic review and meta-analysis. Radiology 2017; 283(3): 692-701.
[http://dx.doi.org/10.1148/radiol.2016161106] [PMID: 27788035]

[234] Leung JWT. MR imaging in the evaluation of equivocal clinical and imaging findings of the breast. Magn Reson Imaging Clin N Am 2010; 18(2): 295-308, ix-x.
[http://dx.doi.org/10.1016/j.mric.2010.02.012] [PMID: 20494313]

[235] Niell BL, Bhatt K, Dang P, Humphrey K. Utility of Breast MRI for further evaluation of equivocal findings on digital breast tomosynthesis. AJR Am J Roentgenol 2018; 211(5): 1171-8.
[http://dx.doi.org/10.2214/AJR.17.18866] [PMID: 30207789]

[236] Berger N, Luparia A, Di Leo G, *et al.* Diagnostic performance of MRI *versus* galactography in women with pathologic nipple discharge: A systematic review and meta-analysis. AJR Am J Roentgenol 2017; 209(2): 465-71.
[http://dx.doi.org/10.2214/AJR.16.16682] [PMID: 28537847]

[237] Das DK, Al-Ayadhy B, Ajrawi MTG, *et al.* Cytodiagnosis of nipple discharge: A study of 602 samples from 484 cases. Diagn Cytopathol 2001; 25(1): 25-37.
[http://dx.doi.org/10.1002/dc.1098] [PMID: 11466810]

[238] Morrogh M, Morris EA, Liberman L, Borgen PI, King TA. The predictive value of ductography and magnetic resonance imaging in the management of nipple discharge. Ann Surg Oncol 2007; 14(12): 3369-77.
[http://dx.doi.org/10.1245/s10434-007-9530-5] [PMID: 17896158]

[239] Panzironi G, Pediconi F, Sardanelli F. Nipple discharge: The state of the art. BJR|Open 2019; 1(1): 20180016.
[http://dx.doi.org/10.1259/bjro.20180016] [PMID: 33178912]

[240] Menezes GLG, Stehouwer BL, Klomp DWJ, *et al.* Dynamic contrast-enhanced breast MRI at 7T and 3T: An intra-individual comparison study. Springerplus 2016; 5(1): 13.
[http://dx.doi.org/10.1186/s40064-015-1654-7] [PMID: 26759752]

[241] Cheshkov S, Dimitrov I, Koning W, *et al.* 2013.https://cds.ismrm.org/protected/ 13MProceedings/files/4407.PDF

[242] van de Bank BL, Voogt IJ, Italiaander M, *et al.* Ultra high spatial and

temporal resolution breast imaging at 7T. NMR Biomed 2013; 26(4): 367-75.
[http://dx.doi.org/10.1002/nbm.2868] [PMID: 23076877]

[243] Sheth KN, Mazurek MH, Yuen MM, *et al.* Assessment of Brain Injury Using Portable, Low-Field Magnetic Resonance Imaging at the Bedside of Critically Ill Patients. JAMA Neurol 2021; 78(1): 41. [http://dx.doi.org/10.1001/jamaneurol.2020.3263]

[244] Matthew S. Rosen (2022) Low-field MRI for Breast Cancer Screening ClinicalTrials.gov Identifier: NCT05486520. 2022.https://clinicaltrials.gov/ct2/show/study/NCT05486520

[245] Hulvershorn J, Borthakur A, Bloy L, *et al.* $T_{1\rho}$ contrast in functional magnetic resonance imaging. Magn Reson Med 2005; 54(5): 1155-62. [http://dx.doi.org/10.1002/mrm.20698] [PMID: 16217783]

[246] Pujara AC, Kim E, Axelrod D, Melsaether AN. PET/MRI in Breast Cancer. J Magn Reson Imaging 2019; 49(2): 328-42. [http://dx.doi.org/10.1002/jmri.26298] [PMID: 30291656]

[247] Melsaether AN, Raad RA, Pujara AC, *et al.* Comparison of whole-body ^{18}F FDG PET/MR imaging and whole-body ^{18}F FDG PET/CT in terms of lesion detection and radiation dose in patients with breast cancer. Radiology 2016; 281(1): 193-202. [http://dx.doi.org/10.1148/radiol.2016151155] [PMID: 27023002]

[248] Orlando A, Dimarco M, Cannella R, Bartolotta TV. Breast dynamic contrast-enhanced-magnetic resonance imaging and radiomics: State of art. Artificial Intelligence in Medical Imaging 2020; 1(1): 6-18. [http://dx.doi.org/10.35711/aimi.v1.i1.6]

[249] Satake H, Ishigaki S, Ito R, Naganawa S. Radiomics in breast MRI: Current progress toward clinical application in the era of artificial intelligence. Radiol Med (Torino) 2022; 127(1): 39-56. [http://dx.doi.org/10.1007/s11547-021-01423-y] [PMID: 34704213]

[250] Bickelhaupt S, Paech D, Kickingereder P, *et al.* Prediction of malignancy by a radiomic signature from contrast agent-free diffusion MRI in suspicious breast lesions found on screening mammography. J Magn Reson Imaging 2017; 46(2): 604-16. [http://dx.doi.org/10.1002/jmri.25606] [PMID: 28152264]

[251] Zhou J, Zhang Y, Chang KT, *et al.* Diagnosis of benign and malignant breast lesions on DCE-MRI by using radiomics and deep learning with consideration of peritumor tissue. J Magn Reson Imaging 2020; 51(3): 798-809. [http://dx.doi.org/10.1002/jmri.26981] [PMID: 31675151]

[252] Chou SHS, Gombos EC, Chikarmane SA, Giess CS, Jayender J. Computer-aided heterogeneity analysis in breast MR imaging assessment of ductal carcinoma *in situ*: Correlating histologic grade and receptor status. J Magn Reson Imaging 2017; 46(6): 1748-59. [http://dx.doi.org/10.1002/jmri.25712] [PMID: 28371110]

[253] Leithner D, Horvat JV, Marino MA, *et al.* Radiomic signatures with contrast-enhanced magnetic resonance imaging for the assessment of breast cancer receptor status and molecular subtypes: Initial results. Breast Cancer Res 2019; 21(1): 106. [http://dx.doi.org/10.1186/s13058-019-1187-z] [PMID: 31514736]

[254] Xiong Q, Zhou X, Liu Z, *et al.* Multiparametric MRI-based radiomics analysis for prediction of breast cancers insensitive to neoadjuvant chemotherapy. Clin Transl Oncol 2020; 22(1): 50-9. [http://dx.doi.org/10.1007/s12094-019-02109-8] [PMID: 30977048]

[255] Cain EH, Saha A, Harowicz MR, Marks JR, Marcom PK, Mazurowski MA. Multivariate machine learning models for prediction of pathologic response to neoadjuvant therapy in breast cancer using MRI features: A study using an independent validation set. Breast Cancer Res Treat 2019; 173(2): 455-63. [http://dx.doi.org/10.1007/s10549-018-4990-9] [PMID: 30328048]

[256] Granzier RWY, van Nijnatten TJA, Woodruff HC, Smidt ML, Lobbes MBI. Exploring breast cancer response prediction to neoadjuvant systemic therapy using MRI-based radiomics: A systematic review. Eur J Radiol 2019; 121: 108736. [http://dx.doi.org/10.1016/j.ejrad.2019.108736] [PMID: 31734639]

[257] Park H, Lim Y, Ko ES, *et al.* Radiomics Signature on Magnetic Resonance Imaging: Association with Disease-Free Survival in Patients with Invasive Breast Cancer. Clin Cancer Res 2018; 24(19): 4705-14. [http://dx.doi.org/10.1158/1078-0432.CCR-17-3783] [PMID: 29914892]

[258] Militello C, Rundo L, Dimarco M, *et al.* 3D DCE-MRI Radiomic Analysis for Malignant Lesion Prediction in Breast Cancer Patients. Acad Radiol 2022; 29(6): 830-40. [http://dx.doi.org/10.1016/j.acra.2021.08.024] [PMID: 34600805]

[259] Prinzi F, Orlando A, Gaglio S, Midiri M, Vitabile S. ML-Based Radiomics Analysis for Breast Cancer Classification in DCE-MRI.Applied Intelligence and Informatics AII 2022 Communications in Computer and Information Science. Cham: Springer 2022; Vol. 1724. [http://dx.doi.org/10.1007/978-3-031-24801-6_11]

[260] Codari M, Schiaffino S, Sardanelli F, Trimboli RM. Artificial Intelligence for Breast MRI in 2008–2018: A Systematic Mapping Review. AJR Am J Roentgenol 2019; 212(2): 280-92. [http://dx.doi.org/10.2214/AJR.18.20389] [PMID: 30601029]